



**TRITON**

Environmental Consultants Ltd.

FISHERIES OCEANOGRAPHY OF THE SOUTHEAST BERING SEA:  
RELATIONSHIPS OF GROWTH, DISPERSION, AND MORTALITY  
OF HERRING LARVAE TO ENVIRONMENTAL CONDITIONS IN  
THE PORT MOLLER ESTUARY

*Prepared under Contract 74-35-0007-30562*

FOR

ENVIRONMENTAL STUDIES UNIT  
Leasing and Environment Office  
Minerals Management Service  
949 E. 36th Avenue, Room 110  
Anchorage, Alaska 99508-4302

PREPARED BY:

Michael McGurk  
David Warburton

John E. Edinger  
Edward M. Buchak



**TRITON**

Environmental Consultants Ltd.

#120 -13511 Commerce Parkway  
Richmond, B.C. Canada V6V 2J1  
Phone: (604) 279-2093  
Fax: (604) 279-2047

**J.E. Edinger Associates, Inc.**

37 West Avenue  
Wayne, Pennsylvania  
19087-3226

Phone: (215) 293-0757  
Fax: (215) 293-0965

July 1991

## Abstract

Five waves of Pacific herring, *Clupea harengus pallasii*, adults entered the Port Moller estuary at intervals of 2-3 wk from late April to mid July, 1990. Each wave split into two groups of spawners, one moving to the head of Moller Bay and the other to the head of Herendeen Bay. Spawning occurred soon after each group reached the head of their bay. The spawning events only lasted 1-2 d, after which the adults left the estuary for offshore summer feeding grounds.

The eggs hatched after 11-25 d of incubation. Larvae were transported seaward at a rate of  $0.8 \text{ km}\cdot\text{d}^{-1}$  in Moller Bay and  $0.5 \text{ km}\cdot\text{d}^{-1}$  in Herendeen Bay. After 10-20 d, seaward advection in both bays stopped when the centroids of the sub-cohorts reached convergence of surface currents, which acted as barriers to seaward transport. Hydrodynamic modelling identified a convergence at Harbor Point in Moller Bay, caused by the collision of seaward baroclinic flow with an anti-seaward upwelling of bottom water, and a convergence at the south end of the deep basin in Herendeen Bay caused by the collision of seaward baroclinic flow with an anti-seaward residual current from Johnston Channel. Centroids of Herendeen Bay sub-cohorts retreated from their convergence at an average rate of  $0.3 \text{ km}\cdot\text{d}^{-1}$ . Centroids of Moller Bay sub-cohorts retreated to a holding area 6 km south of their convergence.

For eight of the nine sub-cohorts the total instantaneous rate of loss of herring larvae,  $0.11 \text{ d}^{-1}$ , was the same as the average rate of mortality, indicating that there was negligible loss of larvae from seaward transport out of the estuary. One sub-cohort from Herendeen Bay had a mortality rate of  $0.05 \text{ d}^{-1}$ , indicating a transport loss rate of  $0.06 \text{ d}^{-1}$ .

All herring larvae were found above the thermocline in the upper 30-40 m. In the deep, stratified water of upper Herendeen Bay, herring larvae exhibited a shallow vertical migration from 0-10 m at night to 10-20 m during the day, but in the shallow, turbulent water of Moller Bay vertical migration was suppressed and larvae were distributed throughout the water column with a concentration close to the sea bottom in the 10-20 m stratum.

Concentrations of prey and predators of herring larvae were always greater in Herendeen Bay than in Moller Bay because the deeper water and lower mixing energy in Herendeen Bay allowed the formation of patches of plankters. Despite this, there was no significant difference between bays in the instantaneous growth of herring larvae, as measured by their RNA-DNA ratio. This suggests that growth was not food-limited.

These results suggest that the Port Moller estuary contains two larval fish retention areas as defined by Iles and Sinclair (1982), and that the population dynamics of Port Moller herring larvae are controlled primarily by hydrodynamic variables that define the retention areas.

## Table of contents

	Page
List of tables	5
List of figures	6
List of appendices	8
1.0 Introduction	9
2.0 Study site	11
3.0 Materials and methods	11
3.1 Physical oceanography	11
3.2 Water circulation modelling	12
3.3 Plankton sampling	13
3.4 Zooplankton analysis	14
3.5 Herring cohort analysis	16
3.6 Herring RNA-DNA analysis	24
4.0 Results	25
4.1 Physical environment	25
4.2 Biological environment	26
4.3 Spawning herring	27
4.4 Herring larval ecology	28
4.4.1 Number and identity of cohorts	28
4.4.2 Age and growth	29
4.4.3 Vertical distribution	30
4.4.4 Dispersion and mortality	31
5.0 Discussion	36
6.0 Conclusions	38
7.0 Acknowledgements	40
8.0 References	40

## List of tables

	Page
Table 1. Distances from plankton stations to the heads of Moller and Herendeen Bays.	49
Table 2. Commercial herring catch in Port Moller, 1982-1990.	50
Table 3. Commercial herring catch and percent roe in Port Moller in 1990.	51
Table 4. Aerial surveys of herring biomass in the Port Moller area in 1990.	52
Table 5. Parameters of Gompertz growth models for eight sub-cohorts of herring larvae.	53
Table 6. Day of year of spawn and day of year of hatch (Do) for nine sub-cohorts of herring larvae.	54
Table 7. Vertical distribution of density of herring larvae at station 36 in Herendeen Bay on June 25-26.	55
Table 8. Vertical distribution of density of herring larvae at station 39 in Moller Bay on July 2.	56
Table 9. Vertical distribution of density of herring larvae at station 36 in Herendeen Bay on July 24-25.	57
Table 10. Locations of the hatch sites of nine sub-cohorts of herring larvae from Port Moller in 1990.	58
Table 11. Mean spatial variance of larval herring density.	58

## List of figures

	Page
Fig. 1. Map of Port Moller estuary with 5 fathom depth contour. Solid circles indicate locations of plankton sampling stations. Boxes indicate stations at which microzooplankton samples were taken, and at which vertically-stratified plankton tows were taken with a Tucker trawl. Stars indicate water pressure sensors. Meteorological data was collected from a station at the tip of Harbor spit. Rainfall data was collected at Entrance Point.	59
Fig. 2. Longitudinal-vertical plot of average water velocities in Moller Bay for May 12-19, 1990.	60
Fig. 3. Longitudinal-vertical plot of average water velocities in Herendeen Bay for May 12-19, 1990.	61
Fig. 4. Length frequency distributions at date for five cohorts of herring larvae found in Port Moller. Each cohort is identified by a circled number and by a broken line connecting mean lengths at date.	62
Fig. 5. Mean lengths ( $\pm 1$ SD) at day of year for nine sub-cohorts of herring larvae. Curves are lengths predicted by Gompertz growth models of Table 5.	63
Fig. 6. Measured density (numbers $\cdot$ m <sup>-2</sup> ) of herring larvae in the Port Moller estuary over May-July, 1990, as measured by bongo nets. Densities are not corrected for extrusion or net avoidance.	64

**List of figures continued**

	Page	
Fig. 7.	Distribution of the ln-transformed factor used to correct densities of herring larvae measured by bongo nets for net avoidance. Corrected-measured ratios are shown for the two mesh sizes of the bongo net.	65
Fig. 8.	The distances from the heads of Moller and Herendeen Bays to the centroids of nine sub-cohorts of herring larvae.	66
Fig. 9.	Regressions of the centroids of eight sub-cohorts of larval herring on shifted age. Shifted age was true age minus the number of days between hatch and maximum distance from the head of a bay that the centroid of a sub-cohort ever reached.	67
Fig. 10.	Plots of ln(density) of herring larvae against the distance between a station and a centroid.	68
Fig. 11.	Change in spatial variance of larval density with age for nine sub-cohorts of herring larvae.	69
Fig. 12.	Plots of ln(density) against age for nine sub-cohorts of herring larvae. Solid lines are predicted ln(density) from equation (15).	70
Fig. 13.	Plots of ln(number) against age for nine sub-cohorts of herring larvae. Solid lines are predicted ln(number) from equation (16).	71

**List of appendices'**

- A. Temperature and salinity profiles in Port Moller in 1990.
- B. Meteorological data from Cold Bay, Alaska.
- c. Hydrographic conditions in the Port Moller estuary in relation to the dispersion and mortality of herring larvae.
- D. Verification of the GLLVHT application to Moller Bay, Alaska
- E. Plankton samples collected in Port Moller in 1990.
- F. Analysis of zooplankton samples from Port Moller in 1990.
- G. Prey and predators of herring larvae in Port Moller in 1990.
- H. Extrusion and avoidance of towed plankton nets by herring larvae.
- I. RNA-DNA analysis of Pacific herring larvae from Port Moller, Alaska.

<sup>1</sup>contained in a separate volume (McGurk et al. 1991)

## 1.0 Introduction

The southeastern Bering Sea is the site of several sac-roe fisheries for Pacific herring, *Clupea harengus pallasii*. It is also a potential site for offshore oil and gas development. Since Pacific herring deposit their eggs in the intertidal and subtidal zones, and their larvae and juveniles rear in coastal embayments, they may be vulnerable to any degradation of the coastal habitat that may be caused by oil and gas development. In response to this concern, the U.S. Minerals Management Service (MMS) began a coastal fishery oceanography study in the southeastern Bering Sea. A one-year pilot investigation of larval herring was conducted in Auke Bay, north of Juneau, Alaska, under an interagency agreement with the U.S. National Oceanic and Atmospheric Administration (NOAA) (McGurk 1989b). That study showed that growth and survival of herring larvae were essentially independent of prey concentration in Auke Bay because prey concentrations were high throughout the May-July study period. This finding was consistent with research that indicates that the mortality of Pacific herring larvae and Atlantic herring, *Clupea harengus harengus*, larvae is a multifactor process involving dispersal and predation as well as starvation (Stevenson 1962; Iles and Sinclair 1982; Moller 1984; Alderdice and Hourston 1985; McGurk 1989a), and that it is not solely determined by the density of food in the first-feeding stage as Hjort (1914) proposed. Based on this finding, McGurk (1989b) recommended that the focus of future work on Alaskan herring larvae should expand to include studies of the dispersal and mortality of herring larvae as well as studies of the trophic relationships of the larvae.

During spring and fall of 1989, MMS funded the collection of oceanographic and meteorological data from the Port Moller estuary (Greengrove 1991). It also supported a brief reconnaissance of the estuary which found there were sufficient numbers of spawning herring to support an intensive study of the population dynamics of their larvae (McGurk 1989c). This reconnaissance was accompanied by a planning study (McGurk et al. 1989), which formed the basis for the 1990 investigations.

This is the draft report of our 1990 investigations. Its objectives were to:

- (a) describe the age, growth, horizontal and vertical distribution of Pacific herring larvae in the Port Moller estuary and the rates of larval advection, diffusion, and mortality;
- (b) describe the biological habitat of the herring larvae by collecting their micro- and macrozooplankton prey and their invertebrate predators;
- (c) describe the physical habitat of the larvae by measuring water pressure, temperature and salinity, and wind speed, wind direction, air temperature, rainfall, and cloud cover;
- (d) describe the time-varying three-dimensional circulation of water within the estuary using a numerical hydrodynamic model;
- (e) test hypotheses of the physical and biological mechanisms responsible for transport and retention of herring larvae in Port Moller by simulating larval transport with the hydrodynamic model; and
- (f) identify the key biological and physical factors responsible for controlling growth, mortality and dispersal of herring larvae in Port Moller.

Objectives (a)-(d) were completed by May 1990. The synthesis of the results, particularly the transport modelling of herring larvae, is currently in progress.

The main text of this report describes the population dynamics of five cohorts of herring larvae that hatched into the estuary. Appendices to this report are contained in a separate document (McGurk et al. 1991). They describe the hydrodynamic conditions in the estuary (Appendices C and D), the data that was used to drive the hydrodynamic model (Appendices A and B), the numbers and densities of herring larvae that were captured (Appendix E), the composition of the non-herring plankton (Appendix F), the prey and predators of herring larvae (Appendix G), the methods used to correct densities of herring larvae for extrusion through the meshes of the nets and for avoidance of the nets (Appendix H), and the RNA-DNA ratios of herring larvae (Appendix I).

## 2.0 Study site

The Port Moller estuary is the largest embayment on the northern shore of the Alaska Peninsula (Fig. 1). It exchanges water with Bristol Bay, the southeastern part of the Bering Sea. Greengrove (1991) summarized the available information on the physical oceanography and climate of the Bristol Bay-Alaska Peninsula region.

Port Moller estuary has a total surface area of 876 km<sup>2</sup> enclosed in four bays: Mud Bay, Nelson Lagoon, Herendeen Bay and Moller Bay. Only the latter two bays are deep enough to permit the entry of research vessels. At low tides the two former bays are dewatered and the rest of Port Moller can only be navigated through narrow channels that are maintained by strong tidal currents. Herendeen Bay consists of a 100 m deep fjord-like inner bay connected to the estuary entrance by a narrow tidal channel. Moller Bay is also connected to the mouth with a narrow tidal channel, but its inner bay is characterized by shallow mud flats.

Twenty three plankton stations were established in the estuary and occupied at least once each week from April 28 to July 30, 1990 (Fig. 1 and Table 1). Samples of plankton were used to describe the ecology of herring larvae and their biological environment. The physical environment was described from temperature and salinity of the water, tide-driven changes in water pressure, and meteorological data.

## 3.0 Materials and methods

### 3.1 Physical oceanography

Depth profiles of temperature and salinity were measured with a conductivity-temperature-depth meter (Seacat profiler, Sea-Bird Electronics Inc., Seattle WA) which was deployed every time a plankton station was occupied. The meter sampled at a rate of 2 records-s<sup>-1</sup>, and since it was dropped at a rate of about 1 m·s<sup>-1</sup>, it recorded data in its internal memory once every 0.5 m. This data was averaged to obtain mean temperature and salinity at 1 m intervals.

Water surface elevation was measured at three locations in the estuary (Fig. 1). At Entrance Point (55°59.2'N 160°34.4'W) a tide gage had been installed by the Cadastral/Coastal Survey Section of the Alaska Department of Natural Resources

(J. Kemmerer, ADNR, Division of Land and Water Management, Anchorage, Alaska, pers. comm.). The elevations it recorded were the primary driving variable of the hydrodynamic model because the vertical location of the gage had been surveyed in reference to mean lower low water. We installed two Anderaa water pressure sensors in the estuary in order to verify the predictions of the hydrodynamic model. One sensor was placed on the boundary of the estuary near plankton station 23 at  $55^{\circ}58.8'N$   $160^{\circ}43.1'W$ , as far from Entrance Point as was possible without entering shallow water. Local pressure effects due to tidal waves entering shallow water were not desirable. A second pressure sensor was placed in the southern end of Herendeen Bay at  $55^{\circ}44.0'N$   $160^{\circ}39.9'W$ , as far as possible from the boundary. The depth of the sensors was not known in relation to mean lower low water, so their data was compared to the model's predictions by comparing the timing and amplitude of water pressure.

An Anderaa meteorological station at Harbor Point ( $55^{\circ}54.8'N$   $160^{\circ}34.7'W$ ) measured wind direction and wind speed every hour. Rain was gaged at the Peter Pan Seafoods Ltd. plant at Entrance Point. Rainfall, dry bulb air temperature, dew point temperature, and the percent of the sky covered with clouds were taken from the records of the Cold Bay airport ( $55^{\circ}12'N$   $164^{\circ}3'W$ ), 50 km west of Port Moller (National Climatic Data Center 1990).

### 3 . 2 Water circulation **modelling**

The hydrodynamics of the Port Moller estuary were computed using the Generalized Longitudinal, Lateral, Vertical, Hydrodynamic and Transport (GLLVHT) model designed by John Edinger and Edward Buchak of J. E. Edinger Associates Inc. A detailed description of GLLVHT was included in the planning study for this project (McGurk et al. 1989). The model was developed from the well-known general three-dimensional and time-varying equations of fluid motion (Edinger and Buchak 1980; Buchak and Edinger 1984). GLLVHT and its earlier versions have been used to model water circulation in over 20 different marine and freshwater environments, e.g. Buchak and Edinger (1984), Edinger and Buchak (1988) and Edinger et al. (1989).

GLLVHT is a boundary-condition model driven by water surface elevation and temperature and salinity at the northern boundary of the estuary, the line from

Entrance Point to Point Edward. Once the model is started computations of water properties, e.g. horizontal and vertical water velocity, salinity, and temperature, proceed inwards from the boundary and are modified by bathymetry, fresh water inflow at the head of the Moller and Herendeen Bays, wind stress, and solar heating. For this reason, the longitudinal predictions of the model are presented with the boundary as the origin. Computations were performed at time steps of 2-15 min. The model was verified by comparing the observed and predicted temperatures and salinities, and by comparing predicted water surface elevations at the western end of the boundary and at the head of Herendeen Bay with the water pressures measured by the two Anderaa sensors.

The bathymetry of the Port Moller estuary was taken from marine chart 16363 published by NOAA. The estuary was represented in GLLVHT as a three-dimensional grid with 151 square cells each with a cell length of 2100 m. Each cell was divided into vertical layers 2 m deep. At a water surface elevation of 10 m above mean lower low water there were 4 to 51 vertical layers in each cell.

### 3.3 Plankton sampling

Plankton was sampled with four types of gear. Small bongo nets were used to capture macrozooplankton each week at station 36 in Herendeen Bay and station 39 in Moller Bay (Fig. 1). The mouth diameter of the nets was 20 cm, the length of the nets was 1.5 m and the mesh width was 165  $\mu\text{m}$ . The net was towed at about 1  $\text{m}\cdot\text{s}^{-1}$  in a double oblique pattern from the sea surface to 1-5 m above the sea bottom and back to the surface. The contents of the codends were preserved in 5% seawater formalin. The volume of water filtered by all plankton nets was measured with a General Oceanics flowmeter paced off center in one of the net mouths.

Microzooplankton was captured at the same two stations with a 30 L open-closing water bottle. The bottle was dropped to depths of 10, 20, 30 and 40 m in Herendeen Bay and 5, 10, 15 and 20 m in Moller Bay. The contents of the bottle were filtered through a 25  $\mu\text{m}$  mesh bag and preserved in 5% seawater formalin.

Larger bongo nets were used to measure the density of herring larvae at each of the 23 stations each week from April 28 to July 30. These nets had a 60 cm mouth diameter, a length of 3 m, and a mesh size of either 333 or 505  $\mu\text{m}$ . The 333  $\mu\text{m}$

mesh was used to capture newly-hatched herring larvae and the 505  $\mu\text{m}$  mesh was used to capture mid-size larvae. On several cruises the two mesh sizes were placed together on one frame in order to measure extrusion of herring larvae through the 505  $\mu\text{m}$  mesh. The net was towed at  $1 \text{ m}\cdot\text{s}^{-1}$  in a double oblique pattern from the sea surface to 1-5 m off the sea bottom and back to the surface. Maximum depth of a tow was calculated from the amount of wire released, as measured with a meter block, and the average angle of the wire, as measured with an inclinometer. The actual depth of the water was known at all times from a depth sounder. The catch was preserved in 5% seawater formalin.

An open-closing Tucker trawl was used to measure the vertical distribution of herring larvae at the same two stations at which zooplankton was sampled. At three dates the trawl sampled 10 m deep strata from the sea surface to the sea bottom every 6 h over a 24 h period. Herendeen Bay was 80 m deep, so 8 strata were sampled once every 6 h, but Moller Bay was only 30 m deep, so only 3 strata were sampled. The trawl had a square mouth with a side length of  $1 \text{ m}^2$  and its net was 3 m long and had a mesh size of 505  $\mu\text{m}$ . It was lowered to the mid-point of a 10 m deep stratum, opened with a messenger, towed at a speed of about  $1 \text{ m}\cdot\text{s}^{-1}$  for 10 min, closed with a second messenger and then retrieved. The net was washed down and all plankton was immediately preserved in 5% seawater formalin. After a sample had been collected the direction of the research vessel was reversed and it retraced its path while the next sample was being collected. This meant that the average current velocity over a series of 6-8 tows was approximately zero.

A Methot trawl was used to capture larger herring larvae (Methot 1986). It had a rigid square mouth with a side length of 1.5 m, a net length of 10 m and a mesh width of 1000  $\mu\text{m}$ . It was towed at about  $1 \text{ m}\cdot\text{s}^{-1}$  in a double oblique pattern from the sea surface to 1-5 m off the sea bottom and back. A 60 cm bongo net tow was done at the same station within 10 min of a Methot trawl tow in order to compare densities and lengths of herring larvae.

### 3.4 Zooplankton analysis

All micro- and macrozooplankton samples were identified and enumerated by Moira Galbraith of Sy-Tech Research Ltd. (Sidney, B.C.). Samples were first washed through a 40  $\mu\text{m}$  sieve in order to remove formalin. Very few organisms

other than diatoms passed through the sieve. The sample was scanned for exotic taxa which, if present, were removed for closer study. Then, the sample was split to a size of approximately 250 individuals and all were identified and enumerated to genus, species, sex and developmental stage. Copepod nauplii and copepodites were separated into four length categories:  $<0.2$ ,  $0.2-0.4$ ,  $0.4-0.6$  and  $>0.6$  mm, before enumeration. Maximum and minimum lengths and widths were measured for each taxon. Density of microzooplankton was calculated as the number $\cdot$ m<sup>-3</sup> of water filtered from the water bottle, and density of macrozooplankton was calculated as the number $\cdot$ m<sup>-2</sup> of sea surface by multiplying number $\cdot$ m<sup>-3</sup> by maximum depth (m) of the tow.

Animals smaller than about 0.4 mm in minimum length were extruded through the meshes of the 165 $\mu$ m net (M. Galbraith, Sy-Tech Research Ltd., pers. comm.). Therefore, the densities of all organisms shorter than 0.4 mm in minimum length were taken from the microzooplankton samples collected by the water bottle, and the densities of all zooplankters with minimum lengths equal to or longer than 0.4 mm were taken from the macrozooplankton samples collected by the 165  $\mu$ m net.

The first step in converting the list of zooplankton into a prey field for herring larvae was to remove all taxa that are rarely eaten by herring larvae because they are too large to fit inside the mouth. Checkley's (1982) laboratory feeding experiments with Atlantic herring larvae showed that the maximum width of prey was 0.51 mm. McGurk's (1989b) review of the diet of Pacific herring larvae captured in the Strait of Georgia and Saanich Inlet, British Columbia, showed that the maximum prey length was 1.4 mm.

The second step was to exclude all other taxa that have rarely ever been observed in the guts of wild herring larvae. Tintinnids, foraminifera, several species of chelicerates and barnacle larvae were excluded from the microzooplankton, leaving a microzooplankton prey field consisting of small and mid-size copepod nauplii, small copepodites, small and mid-size bivalve and gastropod veligers, trochophore larvae, euphausiid protozoa, and small eggs. All jellyfish, flatworms, chaetognaths, juvenile decapods, amphipods, mysids, cumaceans, and the larvae of echinoderms, tunicates, bryozoans, polychaetes and fish were excluded from the macrozooplankton, leaving a macrozooplankton prey field consisting of large

copepod nauplii and copepodites, large bivalve and gastropod veligers, nine species of adult copepods, and euphausiid nauplii.

Densities (number·m<sup>-3</sup> or number·m<sup>-2</sup>) of prey were converted to concentrations (mg dry weight·m<sup>-3</sup> or mg·m<sup>-2</sup>) of prey. This was necessary because densities of different organisms could not be simply added together - there were too many differences in size between prey types. They could only be combined using the common currency of biomass. Concentrations were calculated by multiplying densities of each type of prey by its average weight estimated from weight-length relationships taken from the scientific literature. Average weights of copepods, cladocerans and euphausiid nauplii were estimated from Pearre's (1980) equation for marine copepods. Wet fixed weight was converted to dry fixed weight by assuming a water content of 80%. Dry fixed weight was converted to dry live weight using Giguere et al.'s (1989) equation. Average weight of bivalve and gastropod veligers was estimated from Holland and Spencer's (1973) weight-length relationship for oyster, *Ostrea edulis*, larvae. It was assumed that the length of veligers was not substantially changed by fixation. Average weight of eggs and trochophore larvae was estimated with the equation for an ellipsoid. Wet weight was the product of volume and a specific gravity of 1 mg·mm<sup>-3</sup>, and dry weight was calculated by assuming an 80% water content.

Two classes of invertebrate predators of herring larvae were identified from the macrozooplankton: jellyfish and the chaetognath *Sagitta elegans*. Densities of predators were converted from number·m<sup>-3</sup> to numbers·m<sup>-2</sup> sea surface by multiplying by the depth of the tow.

### 3.5 Herring cohort analysis

All fish larvae were sorted from the other zooplankton in every plankton sample captured with a 333, 505 or 1000µm mesh net. If a sample contained high densities of fish larvae, then it was repeatedly split with a Folsom splitter until a manageable fraction was obtained. All herring larvae were separated from the other species of fish and counted.

Fifty herring larvae were randomly chosen from each sample and their standard lengths were measured to the nearest 0.1 mm. If a larva retained a yolk

sac, then the length and height of the sac were measured to the nearest 0.01 mm and yolk sac volume was estimated with the equation for an ellipsoid.

### Identification of cohorts

Length frequency plots for each sample were used to identify the number of cohorts at each site and date, and to assign each measured larva to a cohort. Assignment was verified by plotting length against date for each cohort and reassigning any outlying larvae to appropriate cohorts. It was checked again by plotting the fraction of larvae that carried a yolk sac against date for each cohort separately and reassigning any outliers.

Each herring larva was then assigned to a sub-cohort based on its location of capture. As a general rule, samples captured in Herendeen Bay, including samples taken at station 27 off Point Divide, were assigned to the Herendeen Bay sub-cohorts and all other samples were assigned to the Moller Bay sub-cohorts. The dividing line between Moller and Herendeen Bays was the Deer Island-Point Divide boundary. This division corresponds to a real spatial separation of sub-cohorts. The internal consistency of sub-cohort assignment was checked by plotting  $\ln(\text{larval density})$  against the square of the distance between a station and its center of population or centroid. Samples that had been assigned to the wrong sub-cohort were clearly visible as outliers with extraordinarily high values of squared residual distance. An iterative process of re-assigning samples to sub-cohorts and replotting  $\ln(\text{density})$  against squared residual distance showed that Herendeen Bay larvae were restricted to that bay, and that Moller Bay larvae were restricted to inner and outer Moller Bay. This conclusion is supported by the distribution of horizontal water velocities predicted by the GVLLHT water circulation model, which showed that Herendeen Bay has a lower flushing rate than Moller Bay.

### Age and growth

Age of herring larvae was calculated as the number of days from the mean date of hatch. Two independent methods were used to estimate the mean dates of hatch. The first method was to backcalculate the date of hatching from a modified Gompertz growth model fit to the lengths at date

$$(1) \quad L_D = L_0 \exp\left[\frac{A_0}{a}(1 - \exp[-a(D - D_0)])\right]$$

where  $L_D$  = length (mm) at day of the year  $D$ ,  $L_0$  = fixed length (mm) at hatch,  $A_0$  = rate of growth ( $\text{mm}\cdot\text{d}^{-1}$ ) at hatch,  $a$  = rate of change ( $\text{mm}\cdot\text{d}^{-1}$ ) of  $L$  and  $D_0$  = day of hatch.  $L_0$  was estimated by regressing mean length against the fraction of yolk sac larvae for all samples that contained at least one yolk sac larva. The modified Gompertz model was fit to mean length at date with non-linear regression.

The second method was based on the number of days from hatching to exhaustion of yolk. Alderdice and Velsen (1971) reported times to yolk exhaustion for 12 combinations of salinity and temperature. The best relationship of these times with temperature was

$$(2) \quad Y = 40.9T^{-0.84}$$

where  $Y$  = time from hatching to yolk exhaustion (d) and  $T$  = mean depth-integrated water temperature ( $^{\circ}\text{C}$ ) (McGurk 1989c; McGurk et al. 1990). Therefore, the mean age of a sample containing at least one yolk sac larva is

$$(3a) \quad t = 40.9T^{-0.84}(1 - f)$$

where  $t$  = age (d) of sample and  $f$  = fraction of yolked larvae in the sample. In this report, we increased the accuracy of this estimator by substituting the ratio of the mean yolk volume of a sample,  $V_y$  ( $\text{mm}^3$ ), to the maximum possible yolk volume,  $V_{y,\text{max}}$  ( $\text{mm}^3$ ), for the fraction of yolked larvae, i.e.

$$(3b) \quad t = 40.9T^{-0.84}\left(1 - \frac{V_y}{V_{y,\text{max}}}\right)$$

The hatch date of a cohort was the mean date at capture minus the mean age of a sample estimated from equation (3b), weighted by the number of larvae measured from the sample, i.e.

$$(4) \quad D_0 = \frac{\sum_i n_i (D_i - t_i)}{\sum_i n_i}$$

where  $n_i$  = number of measured larvae of sample  $i$  collected on day of the year  $D_i$ , and  $t_i$  = mean age (d).

### Tucker trawl catches

Densities of larvae measured with a Tucker trawl were reported as number·m<sup>-3</sup> of water filtered by the net. Densities of larvae in a sample were not divided into densities for each of the five sub-cohorts. However, they were standardized for night-day differences in matchability of the trawl. As described in section H2.1 of Appendix H, the night-day catch ratio of the trawl at the deep, stratified station 36 in Herendeen Bay increased with increasing length of larvae, exceeding a value of 12 for larvae longer than 22 mm. However, there were no night-day differences in matchability at the shallow, well-mixed station 39 in Moller Bay. The most likely cause for this difference in matchability between stations was greater turbidity at station 39 than at station 36. Turbidity suppresses avoidance behaviour by reducing the time available to a fish larvae to detect and avoid an approaching net. In the absence of a direct measure of turbidity, we assumed that it was proportional to the amount of mixing energy in the water which we measured with root mean square water velocity

$$(5) \quad u_{rms} = t_p^{-1} \int U^2(t) dt$$

where  $U_{rms}$  = root mean square velocity (m<sup>2</sup>·s<sup>-1/2</sup>),  $t_p$  = duration (s) of a single  $M_2$  tidal cycle, and  $U(t)$  = depth-averaged water velocity (m·s<sup>-1</sup>) at time  $t$  (s).  $U_{rms}$  was 85 m<sup>2</sup>·s<sup>-1/2</sup> at station 39, but only 2 m<sup>2</sup>·s<sup>-1/2</sup> at station 36. A multiple regression of ln(night-day catch ratio) on larval length,  $L$  (mm), and  $U_{rms}$  [equation (H2)] explained 55% of the variance in ln(ratio). Rearranging equation (H2) gave

$$(6) \quad N = N_0 \cdot 4.118 \cdot 10^{-2} \exp(0.2486L + 3.124 \cdot 10^{-2} U_{rms} - 2.547 \cdot 10^{-3} L \cdot U_{rms})$$

where  $N$  = corrected daytime density (m<sup>-3</sup>) and  $N_0$  = measured daytime density (m<sup>-3</sup>). Densities measured at night did not require correction.

Following Heath et al. (1988), Stephenson and Power (1988) and Munk et al. (1989), the analysis of vertical distribution of herring larvae was based on a division of herring larvae into three length groups: <9.0, 9.0-14.9 and > 15.0 mm. Pooling

densities into size groups was necessary for analysis of variance and it is also a convenient way of showing the data. The depth of the center of mass of the larvae,  $Z_{cm}$ , was calculated as

$$(7) \quad Z_{cm} = \sum^i p_i z_i$$

where  $p_i$  = the proportion of larvae for one series of tows occurring at depth  $i$ , and  $z_i$  = sample depth (m).

### Bongo net catches

Density of larvae captured by the bongo nets was calculated as the number·m<sup>-2</sup> of sea surface by multiplying density (number·m<sup>-3</sup>) by the maximum depth (m) of the tow. Density of a sample measured by a bongo net was then divided into densities of its constituent sub-cohorts by, first, distributing it among 0.5 mm wide larval length bins in amounts proportional to the number of larvae in each bin, and then summing the densities of the bins inside length ranges assigned to each sub-cohort. The procedure was simple for samples in which the length ranges of sub-cohorts did not overlap, but it had to be modified for samples with overlapping length ranges. In those samples, the density of a single length bin within a zone of overlap was partitioned into densities of two or more sub-cohorts by extrapolating the length distribution of each sub-cohort through the bin. All length distributions were assumed to be normally distributed.

Densities of larvae <7.9 mm long that were caught by the 505µm mesh bongo net were multiplied by 3.656 to correct for losses due to extrusion through the net (section H1.0 of Appendix H). There was no significant extrusion of larvae through the 333 µm mesh.

All densities of herring larvae were then corrected for net avoidance. This was an essential step because, as described in section H2.3 of Appendix H, avoidance of towed plankton nets by herring larvae is a serious obstacle to estimating the true density of herring larvae >10 mm long. It can cause 20-40 fold underestimation of density of herring larvae >20 mm long that are caught with a net towed at 1000 mm·s<sup>-1</sup>, the average tow speed used in this study. However, we had no

night-day catch ratios for bongo nets for Port Moller, and we were reluctant to use only the night-day catch ratios from Tucker trawls because of the possibility of bias due to gear-related differences in matchability. We were also reluctant to use a theoretical model of matchability such as that described by Ware and Lambert (1985) for Atlantic mackerel, *Scomber scombrus*, larvae, or to use night-day catch data for species other than herring. Our compromise solution to the problem was to manufacture a general model of net avoidance from a review of the scientific literature on night-day catch ratios of Pacific and Atlantic herring larvae. This review identified larval length, towing speed, and mesh width as the most important factors controlling differences in night-day matchability. The multiple regression model was

$$(8a) \quad N_L = N_{0L} \exp(0.5673 + 0.2408L - 4.097W - 6.664 \cdot 10^{-5}v)L)$$

where  $h_L^T$  = corrected daytime density (number·m<sup>-2</sup>) in a length bin with a mid-point of length L (mm),  $N_{0L}$  = measured daytime density (number·m<sup>-2</sup>) at length L, W = mesh width (mm) and v = tow speed (mm·s<sup>-1</sup>).

From analyses of the Tucker trawl catches we expected additional variation in catchability of the bongo net due to variation in turbidity within the estuary. In the absence of any information on the relationship between matchability of bongo nets and turbidity, we assumed that it is independent of gear type. This allowed us to include in equation (8a) the rate of increase of the intercept of the regression of ln(night-day catch ratio) on length with  $U_{rms}$ , and the rate of decrease of the slope of the regression of ln(ratio) on length with  $U_{rms}$ , that were measured for the Tucker trawl by equation (6), i.e.

$$(8b) \quad N_L = N_{0L} \exp(0.5673 + 0.2408L - 4.097W - 6.664 \cdot 10^{-5}v)L + 3.124 \cdot 10^{-2} U_{rms}^2 - 2.608 \cdot 10^{-3} U_{rms} \cdot L).$$

The result of incorporating  $U_{rms}$  into equation (8) is essentially conservative because it reduces the correction of density of bongo net catches for net avoidance for those regions of the estuary, such as outer Moller Bay, with high turbidity.

### Method trawl catches

Density of herring larvae measured by the Methot trawl were calculated as number·m<sup>-2</sup>. Density was not divided into densities of constituent sub-cohorts, and it was not corrected for extrusion or net avoidance. Methot trawl catches were used only as an independent measure of the matchability of the bongo net (Appendix H). They were not included in the data set used to estimate growth, dispersion, and mortality of herring larvae because too many small larvae were extruded through the 1000 μm mesh for these catches to be useful in that analysis.

### Advection and diffusion

In order to describe the advection and diffusion of larvae within the estuary, distances were assigned to each sampling station by creating a one-dimensional coordinate system for each bay (Table 1). Since herring larvae hatched in the upper half of the estuary, the origins of the systems were placed at the heads of the two bays: the mouth of Portage Creek in Herendeen Bay, and the midpoint of the entrance to the Frying Pan in Moller Bay. Distances of sampling stations to their respective origins were estimated by following straight lines between stations. As a general rule, the lines followed the deep channels. The exception was the straight line between station 38 and 26, which crossed a long stretch of shallow water.

The centers of larval distribution or centroids were calculated as

$$(9) \quad x_t = \left( \sum_i N_{it} X_i \right) / \sum_i N_{it}$$

where  $x_t$  = distance (m) of a centroid of sub-cohort from the origin of the coordinate system in either Moller or Herendeen Bays,  $N_{it}$  = density (m<sup>-2</sup>) of larvae at station  $i$  at age  $t$  (d), and  $x_i$  = distance (m) from the local origin to station  $i$ . Centroids were calculated for each complete survey of the estuary, which in some cases took several days to complete, so the mid-point of the ages of larvae during the survey period was used as an estimate of age. Centroids were only calculated for those sub-cohorts for which there were at least three densities in a survey.

Horizontal spatial variance of larval density,  $s_{xt}^2$  (m<sup>2</sup>), was calculated as

$$(10) \quad s_{xt}^2 = \frac{\sum_i N_{iD}(x_{Di} - x_D)}{\sum_i N_{Di}}$$

Variances were calculated only for surveys that had at least three densities.

### Loss and mortality

Since the instantaneous loss of herring larvae includes loss due to transport of larvae out of the estuary as well as loss due to mortality, the calculation of larval mortality required adjusting larval density to account for loss due to dispersion. We used a population model that incorporated advection, diffusion and mortality. It was based on models described by Okubo (1980), McGurk (1989a, 1989b, 1989c) and McGurk et al. (1990). It has the form

$$(11a) \quad N(x,t) = \frac{M}{\pi s_{xt}^2} \exp\left[-\frac{(x - x_t)^2}{s_{xt}^2} - Zt\right]$$

where  $N(x, t)$  = larval density ( $m^{-2}$ ) at distance  $x$  (m) of a station from its origin and age  $t$  (d),  $M$  = number of herring larvae released into the water at age 0,  $x_t$  = centroid (m) at age  $t$ , and  $Z$  = coefficient of mortality ( $d^{-1}$ ). The model was fit to the data by, first, converting all larval densities to larval numbers by rearranging equation (11a) so that all terms related to dispersion were placed on the left-hand side of the equation, i.e.

$$(11b) \quad n(t) = N(x,t) \cdot \pi \cdot s_{xt}^2 \exp\left[\frac{(x - x_t)^2}{s_{xt}^2}\right]$$

where  $n(t)$  = number of herring larvae at age  $t$ .  $n(t)$  was calculated for each  $N(x,t)$  using the average values of  $x_t$  and  $s_{xt}^2$  that were appropriate for that sub-cohort, bay, position and age.  $x_t$  for each sub-cohort was calculated from the estimated hatch site and the average seaward and anti-seaward advection rates for that date and sub-cohort.  $s_{xt}^2$  for each of the four combinations of bays and position were used. Then,  $n(t)$  was transformed with natural logarithms and regressed on age, i.e.

$$(12) \quad \ln[n(t)] = \ln(M) - Zt.$$

Analyses of the dynamics of the nine sub-cohorts of herring larvae included multiple regression with dummy variables for the sub-cohorts. The dummy variables had the following names and values:

Sub-cohort	x <sub>1</sub>	x <sub>2</sub>	x <sub>3</sub>	x <sub>4</sub>	x <sub>5</sub>	x <sub>6</sub>	x <sub>7</sub>	x <sub>8</sub>	x <sub>9</sub>
1M	1	0	0	0	0	0	0	0	0
1H	0	1	0	0	0	0	0	0	0
2M	0	0	1	0	0	0	0	0	0
2H	0	0	0	1	0	0	0	0	0
3M	0	0	0	0	1	0	0	0	0
3H	0	0	0	0	0	1	0	0	0
4M	0	0	0	0	0	0	1	0	0
4H	0	0	0	0	0	0	0	1	0
5M	0	0	0	0	0	0	0	0	1

### 3.6 Herring RNA-DNA analysis

Every week, 60 cm bongo nets were used to capture 10-30 herring larvae at stations 36 and 39 for RNA-DNA analysis. Larvae were picked from the fresh zooplankton immediately after opening the codend of the net, placed in numbered plastic vials which were then frozen immediately in liquid nitrogen. The vials were transported in their refrigerated flasks to W. Kusser at Microtek Research and Development Ltd. of Sidney, B. C., who stored them at -75°C. Individual larvae were thawed and their length measured to the nearest 0.1 mm. Yolk sac length and height were measured to the nearest 0.01 mm. Concentrations of whole-body RNA and DNA were measured with Clemessen's (1988) method and are expressed as  $\mu\text{g}\cdot\text{fish}^{-1}$ . All statistical analyses were done with ln-transformed RNA and DNA concentrations and RNA-DNA ratios.

## 4.0 Results

### 4.1 Physical environment

In this section, we briefly review the most important findings of our investigations on physical oceanographic features of the Port Moller estuary. Detailed analyses are shown in Appendices A-D.

A total of 310 profiles of temperature and salinity were taken from April 30 to July 29, 1990. The tide gage at the Peter Pan Seafoods plant at Entrance Point was operational from April 30 to July 27, 1990. The water pressure sensor at the bottom of Herendeen Bay was deployed on May 8, 1990, and retrieved on July 20, 1990, and the water pressure sensor at the western end of the estuary's boundary was deployed on May 9, 1990, and retrieved on July 20, 1990. The meteorological station at Harbor Point was installed on May 4, 1990, and removed on July 20, 1990. All four sensors recorded uninterrupted time-series.

Temperature-salinity profiles showed that water was well mixed at the coastal boundary of the estuary, throughout Moller Bay, and in Johnston Channel, but that it was stratified in the deep basin of Herendeen Bay (Appendix A). The thermocline in the deep basin occurred at a depth of 30-40 m.

The numerical model showed that the hydrodynamics of the estuary were dominated by the interaction of tides and bathymetry (Appendix B). Thus, flushing rates were highest near the boundary and decreased with distance from the boundary. The lowest rates of flushing were found at the head of Herendeen Bay. Baroclinic flow due to the seaward movement of freshwater along the surface was less pronounced in 1990 than in 1989 due to lower precipitation in 1990 than in 1989. Wind stress and solar heating had minor effects on hydrodynamics relative to the effects of tides and freshwater inflow.

The most significant finding of the numerical model was the identification of two regions of convergence, one just south of Harbor Point at the junction of outer and upper Moller Bay, and another near Shingle Point where Johnston Channel debouches into the deep basin of Herendeen Bay (Figs. 2 and 3 and Appendix B). These convergence remained stable and intact throughout the May-July study

period. We believe that they are responsible for retaining herring larvae, and perhaps other species of fish larvae, within the estuary. As we will show in section 4.4.4 of this report, the centroids of the nine sub-cohorts of herring larvae always stayed anti-seaward of these convergence, as if the convergence were physical barriers to their seaward transport.

The Moller Bay convergence is caused by the collision of a weak seaward flow of brackish surface water with a strong anti-seaward flow due to upwelling of bottom water. The Herendeen Bay convergence is due to the collision of a weak seaward flow of brackish surface water with an equally weak anti-seaward flow of surface water from Johnston Channel. The seaward flows in both convergence are clearly baroclinic. The origins of the anti-seaward flows are not well understood, although upwelling in Moller Bay is probably caused in some manner by tidal forcing of water through the narrow channel west of Harbor Point. The position of the Moller Bay convergence is unlikely to vary between years because it is dominated by upwelling and not by baroclinic flow. However, we speculate that the position of the Herendeen Bay convergence may vary between years due to variation in freshwater inflow.

#### 4.2 Biological environment

The concentration of prey for herring larvae was greater at station 36 in Herendeen Bay than at station 39 in Moller Bay at almost all dates and over almost all length ranges of herring (Appendix G). The difference was due to differences in water depth and water velocity between stations. Mixing energy at the deep station 36 was much lower than mixing energy at shallow station 39, low enough to allow zooplankton at station 36 to form a scattering layer at a depth of about 30 m that was often dense enough to appear as a false bottom on sonar.

The concentration of microzooplankton prey for herring larvae decreased exponentially with depth in both Moller and Herendeen Bays. Thus the best conditions for feeding of young larvae were always found close to the surface.

The difference in prey concentration between bays and over the study season was not reflected in the RNA-DNA ratios of herring larvae (Appendix I). RNA-

DNA ratio, an index of instantaneous growth, increased with size of herring larvae, but it did not vary with station, prey concentration, temperature, or day of the year.

Jellyfish and the chaetognath *Sagitta elegans* were the two major invertebrate predators of herring larvae (Appendix G). Station 36 in Herendeen Bay always had 5-10 times greater concentrations of both types of predator than station 39 in Moller Bay. This was due to the greater water depths and lower mixing energy at station 36 than at station 39. At station 36, the greatest concentrations of both jellyfish and *S. elegans* were found at and below the thermocline at 30 m, which suggests that herring larvae may have been able to reduce their mortality from these predators by staying above the thermocline.

In summary, the concentrations of prey and predators were both strongly influenced by the depth of the water and by the amount of mixing energy in the water. Prey concentration was always greater in Herendeen Bay than in Moller Bay, but the same lack of turbulence that allowed patches of prey to form also allowed patches of invertebrate predators to form. We can only speculate at the tradeoffs for herring larvae. Despite the differences in prey concentration between bays there were no differences in instantaneous growth. Therefore, we conclude that there was little or no food limitation of herring larval growth in the Port Moller estuary over May-July, 1990.

#### 4\*3            Spawning herring

A small herring fishery has occurred in the Port Moller area every year since 1982, catching an average of  $505.5 \text{ t yr}^{-1}$  for the Japanese sac roe market (Table 2). About one third of the catch was taken in Herendeen Bay and near Deer Island, one third in Moller Bay and the remaining third on the Bering Sea coast near Bear River. According to the management plan of the Alaska Department of Fish and Game (ADF&G), this catch is less than or equal to an annual harvest of 20% of the total spawning biomass, which implies that about 2,500 t of spawning biomass enters Port Moller each spring.

In 1990, a total of 247.7 t were captured between June 4 and June 19, half of which were taken in Herendeen Bay and the other half in upper Moller Bay (Table 3). The percent of biomass that consisted of sac roe showed only one peak for each

bay: 7.85% on June 5 for Moller Bay and 8.5095 on June 13 for Herendeen Bay. These peaks may represent the eggs that produced the third sub-cohorts of larvae, which were spawned on June 11 in Moller Bay and June 9 in Herendeen Bay (Table 4).

The plankton survey conducted in this study identified five cohorts of herring larvae hatching at intervals of about 2 wk from May 27 to July 24, each of which corresponded to a separate wave of spawners. Why did the sac roe fishery miss four of the five waves of spawners? Finding spawning herring in the Port Moller-Bear River district with aerial surveys is difficult due to poor weather and muddy water. In the nine years that ADF&G has been conducting aerial surveys in Port Moller, only the surveys done in 1989 were considered to provide accurate assessments of total spawning biomass (McCullough 1990). This factor plus the relatively small biomass of herring in Port Moller compared to that of the Togiak district means that commercial fishermen in Bristol Bay are able to make more money with less effort by fishing herring in the Togiak region in May and early June and then switching to salmon and other species after mid-June. The herring fishery of Port Moller has always been a commercial gamble conducted primarily by fishermen returning to their home ports after the Togiak fishery.

ADF&G conducted 12 aerial surveys of the Port Moller-Bear River district from May 21 to June 14 (Table 4). Although the average visibility rating was “good”, the pilot saw a total biomass of only 654 t, much less than the biomass expected from previous years.

#### 4.4 Herring larval ecology

##### 4.4.1 Number and identity of cohorts

Five cohorts of herring larvae hatched into the Port Moller estuary during the May-July period. They were seen as five modes in the length frequency distributions (Fig. 4). Cohorts were numbered from 1 to 5 depending on their hatch dates; the earliest cohort was labelled number 1 and the latest cohort was labelled number 5. Each of the first four cohorts was composed of two sub-cohorts: one sub-cohort that hatched in Moller Bay and a second that hatched in Herendeen Bay about 2 d later. Cohort 5 consisted of a single sub-cohort that hatched in Moller

Bay. Its Herendeen bay counterpart may have existed, but our sampling program ended before it hatched. Each sub-cohort was labelled according to its bay of hatch, e.g. 4M refers to the Moller sub-cohort of cohort 4.

#### 4.4.2 Age and growth

A regression of the mean length,  $L$  (mm), of herring larvae in a sample with the fraction of larvae,  $f$ , in that sample that carried a yolk,

$$(13) \quad L = 9.3 - 1.75f \quad r^2 = 0.46, P < 0.001 \\ (SE) (0.1) (0.4)$$

predicted a length of 7.6 mm when all larvae were yolked. This value of  $L_0$  was used to fit Gompertz growth models to the mean lengths at date for each of the nine sub-cohorts (Table 5, Fig. 5).

The yolk sac stage lasted 1-15 d, with a mean of 7 d (SD = 4, n = 9). Since this is similar to the expected duration of 5-7 d over a temperature range of 8-11°C, we conclude that most of the larvae hatched over 1-2 d, which implies that spawning also occurred over 1-2 d. Maximum yolk volume,  $V_{y,max}$ , was calculated by estimating the yolk volume for the smallest mean length: 7.1 mm. The best fitting regression model was an exponential decay of yolk volume with length

$$(14) \quad \ln(V_y) = 8.5166 - 1.3801L; r^2 = 0.42, P < 0.001. \\ (SE) (1.1871) (0.1637)$$

The predicted  $V_{y,max}$  at a mean length of 7.1 mm was 0.277 mm<sup>3</sup>. In contrast, the predicted  $V_{y,max}$  at a mean length of 7.6 mm was 0.139 mm<sup>3</sup>, which shows that mean yolk volume decreased by 50% while all larvae were still carrying a yolk sac.

Hatch dates calculated from equation (4) were an average of 2 d (SD = 2, n = 8) later than the dates calculated from growth curves (Table 6). Since these two methods were independent of each other, a mean hatch date was calculated for each sub-cohort. Herendeen Bay sub-cohorts hatched an average of 2 d (SD = 3, n = 4) later than their Moller Bay counterparts. The time interval between hatching of cohorts ranged from 11 to 14 d with a mean of 13 d (SD = 2, n = 3).

### Spawning dates

The dates at which the nine sub-cohorts were spawned in the estuary were back-calculated from the mean hatch dates using Alderdice and Jensen's (1971) relationship between percent daily development of Pacific herring eggs and water temperature (Table 6). Surface water temperatures were taken from the plankton station nearest to the spawning site of the eggs. Incubation times ranged from 25 d in early May to 11 d in mid-July.

#### 4.4.3 Vertical distribution

Almost all larvae were captured in the upper 40 m of the water column, with the highest densities occurring in the upper 30 m (Tables 7, 8 and 9). Since the thermocline at site 36 in Herendeen Bay occurred at 30-40 m in June and July and the water column at site 39 in Moller Bay was mixed from top to bottom, we conclude that herring larvae in the Port Moller estuary were restricted to the mixed layer above the thermocline.

At site 36 on June 25-26, the depth of maximum larval density was at its deepest, 10-20 m, during the day and at its shallowest, 0-10 m, during the night and early twilight (Table 7). The same pattern was apparent in both the 9.0-14.9 mm and  $\geq 15.0$  mm length groups. A three-way ANOVA of  $\ln(\text{density})$  on time of day (day-twilight and night), depth (0-10 and 10-20 m) and length (9.0-14.9 mm or  $\geq 15.0$  mm) showed that only the time-depth interaction was significant ( $P = 0.019$ ). This supports the observation of a shallower vertical distribution at night than during the day, and it supports the observation that the daily vertical migration is independent of larval size. Mean  $Z_{\text{cm}}$  for all length classes was 7 m at night and 10 m ( $SD = 2$ ,  $n = 4$ ) during the day.

A similar pattern of shallow distribution at night and deeper distribution during the day was suggested by the densities measured at the same site on July 24-25 (Table 9). For example, maximum densities were found in the 0-10 m depth strata at night and early twilight, but were found in the 10-20 and 30-40 m depth strata during day and late twilight. However, a three-way ANOVA of  $\ln(\text{density})$  on time of day (day-twilight and night), depth (0-10, 10-20, 20-30 and 30-40 m), and

length (9.0-14.9 mm and  $\geq 15.0$  mm) did not support these observations; none of the three factors or their interactions were significant ( $P > 0.05$ ). Therefore, the mean  $Z_{cm}$  for all size classes of larvae at all times of the day was 16 m (SD = 6, n = 4).

In contrast, at site 39 on July 2, larval density tended to increase with increasing depth and there was no indication of a day-night difference in vertical distribution (Table 8). A three-way ANOVA of  $\ln(\text{density})$  on time of day (day-twilight or night), depth (0-10, 10-20 and 20-30 m) and larval length (<9.0 mm, 9.0-14.9 mm and  $\geq 15.0$  mm) showed a highly significant decrease in  $\ln(\text{density})$  with length ( $P < 0.001$ ) and a barely significant decrease in  $\ln(\text{density})$  with depth ( $P = 0.02$ ). This supports the observation that herring larvae were more common closer to the sea bottom than the sea surface at this site, and that there was no strong evidence for a day-night difference in this distribution or for size-dependence of vertical distribution. The mean  $Z_{cm}$  for all length classes at all times of the day was 15 m (SD = 5, n = 8).

These results show that there were two patterns of vertical distribution of herring larvae corresponding to two different physical regimes. In the stratified water column of station 36 of Herendeen Bay, herring larvae were concentrated in the upper 10 m during the night, and they moved into slightly deeper water, 10-20 m, during twilight and daytime. In the very turbulent water column of station 39 in Moller Bay, herring larvae were found throughout the water column, but they were concentrated in the 20-30 m strata close to the sea bottom, and they did not migrate vertically on a daily basis.

#### 4.4.4 Dispersion and mortality

All sub-cohorts of herring larvae hatched in the estuary from sites in inner Moller Bay and near the deep basin at the head of Herendeen Bay (Fig. 6). All sites were north of the surface current convergence in each bay.

#### Correction of bongo net catches for net avoidance

The factor used to correct measured densities of herring larvae collected by the bongo nets ranged from 0 to 14.3 (Fig. 7). This is similar to the range of correction factors used for Atlantic mackerel larvae by Ware and Lambert (1985),

but lower than those used by McGurk (1989a) for Pacific herring larvae, and much lower than those used by Leak and Houde (1989) for bay anchovy, *Anchoa mitchilli*, larvae.

### Advection

The distances of the centroids from the origins of their coordinate systems followed a dome-shaped pattern with age for most sub-cohorts (Fig. 8). Distances increased soon after hatch to a maximum of 24 km in Moller Bay, near station 39, and a maximum of 20 km in Herendeen Bay, near station 29, and then they decreased with age. The age at which maximum distance was reached varied directly with the distance of the hatch site. Cohorts that hatched from sites close to the maximum, e.g. sub-cohort 1M or 2H, reached the maximum distances within 10 d of hatching, but cohorts that hatched from sites far from the maximum, e.g. sub-cohorts 4M and 1H, reached the maximum distances within 10-20 d of hatching.

In order to obtain estimates of the rates of advection towards the maximum distance and away from it, each dome in Fig. 8 was shifted down the age axis so that the maximum distance of each sub-cohort was at zero age. Then the centroids on the left-hand limbs of the curves for each of the two bays were regressed on shifted age. Simple linear regressions fit the left-hand limbs well, explaining 79 to 89% of the data (Fig. 9). The rate of seaward advection in Moller Bay was  $0.8 \text{ km}\cdot\text{d}^{-1}$ , 50% higher than the rate in Herendeen Bay, but this difference was not statistically significant ( $P > 0.05$ ). The mean distance that Moller Bay centroids reached before beginning their anti-seaward movement was 21.4 km (SD = 3.5,  $n = 4$ ), mid-way between stations 39 and 41. The mean distance that Herendeen Bay centroids reached was 17.8 km (SD = 3.4,  $n = 4$ ), mid-way between stations 31 and 29. These average distances correspond almost exactly with the positions of the surface convergence described in section 4.1 of this report.

There was no significant regression of distance on shifted age for the right-hand limb of Moller Bay. Centroids remained an average of 15 km (SD = 4,  $n = 14$ ) from the head of Moller Bay, about 6 km anti-seaward of the maximum distance that they reached at a shifted age of zero d. However, distances of Herendeen Bay sub-cohorts decreased with age at a rate of about  $0.3 \text{ km}\cdot\text{d}^{-1}$ , reaching a distance of less than 6 km from the origin in the oldest centroid.

### Hatching sites

The locations of the hatching sites for each of the nine sub-cohorts were estimated by back-calculating from the centroids on the left-hand limbs of the centroid-age curves using the advection rates shown in Fig. 9 (Table 10). All of the hatching sites in Moller Bay occurred between stations 41 and 46, and all of the sites in Herendeen Bay occurred between stations 36 and 31.

### Advection and water velocity

There is strong evidence that the initial seaward advection of the centroids of the nine sub-cohorts was controlled by hydrodynamic variables. The rate at which the centroids were advected seawards was higher in Moller Bay than in Herendeen Bay, a result that would be expected from the higher flushing rates in Moller Bay than in Herendeen Bay. The maximum seaward distances reached by the centroids of the Moller Bay sub-cohorts correspond closely to the position of the strong surface convergence near station 39 that is predicted by the GLLVHT model. The maximum seaward distances reached by centroids of the Herendeen Bay sub-cohorts also correspond closely to the surface convergence between stations 33 and 35 that is predicted by the GLLVHT model.

There is evidence that hydrodynamics were less important to the movement of older larvae than of young larvae, and that the movement of older larvae was dominated by directed movement rather than passive transport. After reaching the surface convergence at the north end of the deep basin of Herendeen Bay, the centroids of the Herendeen Bay sub-cohorts retreated to the head of the Bay at a rate of about  $0.3 \text{ km}\cdot\text{d}^{-1}$ . Even if this movement was accomplished by passively drifting on anti-seaward currents, the vertical movements necessary to locate and stay within this current may have required directed movement by the larvae. The situation was less clear in Moller Bay. After reaching the surface convergence south of Harbor Point, the centroids of the Moller Bay sub-cohorts retreated to a position about 6 km south of the convergence and stayed there for the remainder of the larval stage.

## Diffusion

Plots of  $\ln(\text{density})$  on the distance between stations and their centroids show that the horizontal distribution of herring larvae was symmetrical in the Herendeen Bay sub-cohorts and highly asymmetrical in the first four Moller Bay sub-cohorts (Fig. 10). Presumably, the seaward/anti-seaward difference was greater in Moller Bay than in Herendeen Bay because of the greater degree of tide-induced flushing in Moller Bay than in Herendeen Bay.

The asymmetrical distribution of larval density about the centroid meant that the variances of the seaward and anti-seaward limbs of the distribution had to be calculated separately. A three-way ANOVA of  $s_{xt}^2$  with bay (Moller or Herendeen), position (seaward or anti-seaward), and cohort (1 to 4), and covariates day of year and age showed that  $s_{xt}^2$  varied significantly ( $0.001 < P < 0.01$ ) only with bay, position, and the interaction of bay and position. The significant results were due to the fact that mean  $s_{xt}^2$  of the seaward position of Moller Bay was more than twice as great as mean  $s_{xt}^2$  for the other three combinations of bay and position (Fig. 11, Table 11). The spatial variance of herring larval density was clearly correlated with the degree of tidal flushing of the estuary. The rank order of increasing mean  $s_{xt}^2$ : Herendeen/anti-seaward, Herendeen/seaward, Moller Bay/anti-seaward, and Moller Bay/seaward, is the same rank order of regions of the estuary determined by the rate of tidal flushing.

## Loss of herring larvae

Density ( $\text{number} \cdot \text{m}^{-2}$ ) of herring larvae followed a dome-shaped pattern with age in all sub-cohorts (Fig. 12). In sub-cohorts 2M, 2H, 3M, and 3H, the dome of the catch curve occurred 3-5 d after hatch, but in sub-cohorts 1M, 1H, 4M, and 4H the dome was not reached until ages of 21, 15, 5, and 13 d, respectively. The delays in recruitment were mainly due to the time required by the sub-cohorts to move from the hatch sites on the shelves of Moller and Herendeen Bays out to the plankton stations in the channels.

Covariance analysis was used to estimate the loss of herring larval density with time, and how this varied between sub-cohorts. Only densities for the fully recruited right-hand limbs of the catch curves of each sub-cohort were used. The

regression model that explained the most variance in  $\ln(\text{density})$  ( $r^2 = 0.312$ ,  $n = 378$ ) was

(15)	variable	coefficient	SE	P
	intercept	3.8121	0.1713	<0.001
	age	-0.1089	0.0085	<0.001
	$x_1$	1.0444	0.2969	0.001
	$x_6$	-0.7067	0.2733	0.010

This model shows that herring were lost from all sub-cohorts at an average instantaneous rate of  $0.11 \text{ d}^{-1}$ , and that the density of larvae at the age of full recruitment to the plankton nets was significantly greater for sub-cohort 1M, and significantly lower for sub-cohort 3M, than for the other seven sub-cohorts.

### Mortality

Multiple regression with dummy variables for sub-cohorts was used to compare slopes and intercepts of the regression of larval number on larval age. The regression that explained the most variance ( $r^2 = 0.405$ ,  $n = 378$ ) in  $\ln(\text{number})$  was

(16)	variable	coefficient	SE	P
	intercept	24.1783	0.2192	<0.001
	age	-0.1141	0.0095	<0.001
	$x_1$	2.7054	0.3272	<0.001
	$x_3$	1.7526	0.2480	<0.001
	$x_5$	1.2928	0.2640	<0.001
	$x_6$	-2.0382	0.6336	0.001
	$x_7$	1.0098	0.3063	0.001
	$x_6 \cdot \text{age}$	0.0651	0.0302	0.032

This model shows that mortality of all sub-cohorts except 3H was  $0.11 \text{ d}^{-1}$ , which was not significantly different from the total loss rate estimated by equation (15) (Fig. 13). This implies negligible loss of larvae due to seaward transport in these eight sub-cohorts. Sub-cohort 3H had a significantly lower mortality of  $0.065 \text{ d}^{-1}$ , which implies a loss due to transport from these two sub-cohorts of  $0.05 \text{ d}^{-1}$ .

## 5.0 Discussion

The major finding of the 1990 investigations of herring larvae in the Port Moller estuary was a remarkable spatial coincidence between hydrodynamic features and the distribution of herring larvae. The hatch sites and the centroids of all of the nine sub-cohorts of herring larvae were always found anti-seaward of the two convergence of surface currents, as if the convergence were physical barriers to the seaward transport of herring larvae. This situation closely resembles the “retention zone” or “member-vagrant” hypothesis originally proposed by Stevenson (1962) for Pacific herring and later elaborated by Iles and Sinclair (1982) for Atlantic herring. The central ideas of this hypothesis are that retention zones are physical oceanographic features defined by fronts or convergence, that spawning by herring takes place only inside retention zones, and that herring larvae transported out of a retention zone do not spend enough time in the zone to imprint on it and so they do not return there to spawn. In effect, they are lost to the stock even though they may survive to spawn elsewhere.

All other factors being equal, this hypothesis predicts that the spawning biomass of a stock is limited by the average size of the retention zone, and that recruitment to a stock is controlled by annual changes in the size of the retention zone or in the rate at which herring larvae “leak” from the zone. In the Port Moller estuary, the sizes of the larval herring retention zones in Moller and Herendeen Bays are defined by the seaward extent of the convergence. The Moller Bay convergence is probably fixed in place near Harbor Point because it is caused by upwelling due to an interaction of tides and bathymetry. However, the Herendeen Bay convergence is dominated by baroclinic circulation so it can be expected to move up and down the Bay in response to annual changes in freshwater inflow. In 1989, a year of high precipitation and strong baroclinic flows (McGurk 1989c), the Herendeen Bay convergence may have been pushed as far north as the Deer Island-Point Divide channel, effectively making all of Herendeen Bay a retention zone for herring larvae.

If 1990 was indeed a year of relatively low freshwater input and low baroclinic flows, then we would expect little “leakage” of herring larvae from the two retention zones. The results of the population analysis supports this prediction; the mortality of herring larvae for eight of the nine sub-cohorts,  $0.11 \text{ d}^{-1}$ , was not

significantly different from the total loss rate of  $0.11 \text{ d}^{-1}$ , indicating that leakage was effectively zero for these seven sub-cohorts.

The size of retention zones is not the only factor that maybe responsible for recruitment variation in Port Moller herring; concentrations of prey and predators may also have had an effect. However, there was little evidence of food-limited growth of Port Moller herring larvae in 1990. Average linear growth was  $0.32 \text{ mm} \cdot \text{d}^{-1}$ , which is well within the range expected for populations of Pacific herring larvae (McGurk 1989a,b). RNA-DNA ratios were similar between areas and they were not correlated with prey concentration, which suggests that prey concentration was high enough to saturate feeding of herring larvae. The fact that RNA-DNA ratio increased directly with larval length suggests that larvae may have ascended a learning curve of foraging (Robinson 1988), but at the present time we do not know if the relatively low ratios of young larvae are evidence of starvation. The average mortality of herring larvae in the estuary was only  $0.05\text{-}0.11 \text{ d}^{-1}$ , which is well within the range of mortality reported for other populations of Pacific and Atlantic herring larvae (Stevenson 1962; McGurk 1989b; Fortier and Gagne 1990 and references cited therein), and does not support the hypothesis of catastrophic mortality expected from starvation.

If there is a single conclusion to the 1990 investigations, it is that the dispersion of herring larvae in the Port Moller estuary is strongly influenced by the hydrodynamics of the estuary. If year-class strength of herring is established by the end of the larval stage, then this linkage between dispersion and hydrodynamics may be the single most important mechanism of recruitment in populations of Alaskan herring. Based on this reasoning, our task over the next year is to complete the investigations of dispersal of herring larvae (and sand lance, *Ammodytes hexapterus*, larvae) using the numerical hydrodynamic model. We plan to attack the problem in three steps:

- (1) particle path tracing using passive particles released at fixed depth strata in the model in order to determine the appropriate schedules of choice of depth, and in order to determine at what age fish larvae cease moving like passive particles and began moving with directed motion;

- (2) reproducing the observed distribution of larval densities by simulating the unrestricted horizontal and vertical transport of larvae within the estuary. This will allow us to estimate loss of larvae due to transport from the estuary ; and
- (3) exercising the hydrodynamic model over a wide range of meteorological conditions in order to produce functional relationships between leakage of fish larvae from the retention zones and meteorological variables. These relationships will be the first quantitative predictions of the retention zone theory of year-class formation in Pacific herring larvae.

## 6.0 Conclusions

1. Hydrodynamic modeling of the Port Moller estuary identified two convergence of surface currents, one at Harbor Point in Moller Bay and a second at the south end of the deep basin in Herendeen Bay. Both convergence appear to be barriers to seaward transport of herring larvae. They define retention zones within which adult herring spawn and herring larvae feed and grow.
2. Five waves of spawning adult herring entered the estuary at intervals of 2-3 wk from late April to mid July. Each wave split into two groups; one swam to the head of Moller Bay and the other swam to the head of Herendeen Bay. Each group spawned at locations anti-seaward of the convergence of surface currents.
3. After 11-25 d of incubation, larvae of the nine sub-cohorts (5 waves of spawners x two spawning groups minus one sub-cohort that spawned too late to be sampled) hatched and were transported seaward at a rate of  $0.8 \text{ km}\cdot\text{d}^{-1}$  in Moller Bay and  $0.5 \text{ km}\cdot\text{d}^{-1}$  in Herendeen Bay.
4. Seaward advection ceased 10-20 d after hatching once the centroids of the nine sub-cohorts reached the convergence. Herendeen Bay sub-cohorts then retreated anti-seaward at a rate of  $0.3 \text{ km}\cdot\text{d}^{-1}$ , but Moller Bay sub-cohorts moved to a nursery area about 6 km anti-seaward of the convergence.

5. *The rate of diffusion of larvae from the centroids was proportional to the amount of mixing energy in the water. Spatial variance of larval density followed the same rank order as the rate of flushing predicted by the hydrodynamic model.*
6. Larvae were lost from the sub-cohorts at an average instantaneous rate of  $0.11 \text{ d}^{-1}$ . This loss rate was due entirely to mortality in eight of the nine sub-cohorts. Mortality was probably due mainly to predation. In the other sub-cohort, mortality was  $0.05 \text{ d}^{-1}$ , which suggests that the remaining loss,  $0.06 \text{ d}^{-1}$ , was due to transport of larvae out of the retention zone.
7. *All herring larvae were captured above the thermocline (30-40 m). In stratified water with low mixing energy, such as in the deep basin of Herendeen Bay, herring larvae exhibited a shallow vertical migration from 0-10 m at night to 10-20 m during the day. But in the shallow and well-mixed water of Moller Bay, vertical migration was inhibited and larvae were distributed throughout the water column with a maximum concentration close to the sea bottom in the 10-20 m stratum.*
8. Concentrations of prey for herring larvae and concentrations of their inv.ertebrate predators (primarily jellyfish and *Sagitta elegans*) were always greater in Herendeen Bay than in Moller Bay because the greater depth and lower mixing energy of Herendeen Bay allowed the formation of high-density patches of zooplankters.
9. Concentrations of microzooplankton prey for herring larvae (primarily copepod nauplii) decreased exponentially with depth in both Herendeen and Moller Bays.
10. Despite the differences in prey concentration between Moller and Herendeen Bays, the mean RNA-DNA ratio of herring larvae, an index of instantaneous growth, did not vary between bays. The average linear rate of growth in length of herring larvae,  $0.32 \text{ mm}\cdot\text{d}^{-1}$ , also did not vary between cohorts. This evidence suggests that larvae were not food-limited in either location.

11. We conclude that population dynamics of herring larvae in Port Moller are strongly influenced by the hydrodynamics of the estuary. Numerical modelling of larval herring transport will be performed in 1991 in order to further test this hypothesis.

## 7.0 Acknowledgements

This study was funded by the Alaska Outer Continental Shelf Region of the Minerals Management Service, U.S. Department of the Interior, Anchorage, Alaska, under contract no. 14-35-0001-30562. We gratefully acknowledge the assistance of R. Meyer, L. Jarvela, P. Harmon, J. Dermoty, F. Dyson, R. Baxter, J. McCullough, N. Daboul and S. Clouse. Members of the School of Fisheries of the University of Washington: P. Dinnel, G. Jensen, H. Anderson, J. Orensanz, R. Neimuth, Y. Shi and A. Shaffer, and the captain and crew of the FV Cascade of the Alaska Crab Coalition, assisted in collecting samples. The staff of the Peter Pan Seafoods Ltd. plant at Port Moller, especially D. Lall, M. Persky, and J. Hinsberger, provided logistics support. We thank our sub-contractors: W. Kusser (Microtek Research and Development Ltd.) and M. Galbraith (Sy-Tech Research Ltd.).

## 8.0 References

- Ahlstrom, E. H. 1954. Distribution and abundance of egg and larval populations of the Pacific sardine. U.S. Fish and Wildl. Serv., Fish. Bull. 56:83-140.
- Alderdice, D. F., and A. S. Hourston. 1985. Factors influencing development and survival of Pacific herring (*Clupea harengus pallasii*) eggs and larvae to beginning of exogenous feeding. Can. J. Fish. Aquat. Sci. 42 (Suppl. 1): 56-68.
- Alderdice, D. F., and F. P. J. Velsen. 1971. Some effects of salinity and temperature on early development of Pacific herring (*Clupea pallasii*). J. Fish. Res. Board Can. 28:1545-1562.
- Barraclough, W. E. 1967a. Number, size and food of larval and juvenile fish caught with a two boat surface trawl in the Strait of Georgia April 25-29, 1966. Fish. Res. Board Can. MS Rep. No. 922: 54p.

- Barraclough, W. E. 1967b. Number, size and food of larval and juvenile fish caught with an Issacs-Kidd trawl in the surface waters of the Strait of Georgia April 25-29, 1966. Fish. Res. Board Can. MS Rep. No. 926:79 p.
- Barraclough, W. E. 1967c. Number, size composition and food of larval and juvenile fish caught with a two-boat surface trawl in the Strait of Georgia June 6-8, 1966. Fish. Res. Board Can. MS Rep. No. 928:58 p.
- Barraclough, W. E., and J. D. Fulton. 1967. Number, size composition and food of larval and juvenile fish caught with a two-boat surface trawl in the Strait of Georgia July 4-8, 1966. Fish. Res. Board Can. MS Rep. No. 940: 82p.
- Barraclough, W. E., and J. D. Fulton. 1968. Food of larval and juvenile fish caught with a surface trawl in Saanich Inlet during June and July 1966. Fish. Res. Board Can. MS Rep. No. 1003:78 p.
- Barraclough, W. E., D. G. Robinson, and J. D. Fulton. 1968. Number, size composition, weight, and food of larval and juvenile fish caught with a two-boat surface trawl in Saanich Inlet during April 23-July 21, 1968. Fish. Res. Board Can. MS Rep. No. 1004: 305p.
- Brander, K., and A. B. Thompson. 1989. Diel differences in avoidance of three vertical profile sampling gears by herring larvae. J. Plankton Res. 11:775-784.
- Bridger, J. P. 1956. On day and night variations in catches of fish larvae. J. Cons. int. Explor. Mer 22:42-57.
- Bridger, J. P. 1958. On efficiency tests made with a modified Gulf III high-speed tow net. J. Cons. int. Explor. Mer 23:357-365.
- Buchak, E. M., and J. E. Edinger. 1984. Generalized, longitudinal-vertical hydrodynamics and transport: development, programming and applications. Prepared for the U.S. Army Corps of Engineers, Waterways Experimental Station, under contract DACW39-84-M-1636 by J. E. Edinger Associates, Inc., Wayne, Pennsylvania.

- Checkley, D. M., Jr. 1982. Selective feeding by Atlantic herring (*Clupea harengus*) larvae on zooplankton in natural assemblages. *Mar. Ecol. Prog. Ser.* 9:245-253.
- Clemessen, C. M. 1988. A RNA and DNA fluorescence technique to evaluate the nutritional condition of individual marine fish larvae. *Meeresforsch.* 32:134-143.
- Clutter, R. I., and M. Anraku. 1968. Avoidance of samplers, p. 57-76. In D. J. Tranter [ed.] Part 1. Reviews on zooplankton sampling methods. UNESCO Monogr. Oceanogr. Methodol. 2. Zooplankton sampling.
- Coachman, L. K., and R. L. Charnell. 1977. Fine structure in outer Bristol Bay, Alaska. *Deep Sea Res.* 24:869-889.
- Cohen, R. E., and R. G. Lough. 1983. Prey field of larval herring (*Clupea harengus*) on a continental shelf spawning area. *Mar. Ecol. Prog. Ser.* 10:211-222.
- Colton, J. B., Jr., K. & Honey, and R. F. Temple. 1961. The effectiveness of sampling methods used to study the distribution of larval herring in the Gulf of Maine. *J. Cons. int. Explor. Mer* 26:180-190.
- Colton, J. B., Jr., J. R. Green, R. R. Byron, and J. L. Frisella. 1980. Bongo net retention rates effected by towing speed and mesh size. *Can. J. Fish. Aquat. Sci.* 37:606-623.
- Edinger, J. E., and E. M. Buchak. 1980. Numerical hydrodynamics of estuaries in estuarine and wetland processes with emphasis on modelling. p. 115-146 In Hamilton, P., and K. B. MacDonald [eds.], Plenum Press, New York, N.Y.
- Edinger, J. E., and E. M. Buchak. 1988. Larval transport and entrainment modelling for the Patuxent estuary and Chalk Point Steam Electric Station. Prepared for Potomac Electric Power Company, Environmental Affairs Group, Water and Land Use Department, Washington, D. C., by J. E. Edinger Associates, Inc., Wayne, Pennsylvania.

- Edinger, J. E., E. M. Buchak, and N. C. Huang. 1989. Chalk Point Steam Electric Station Patuxent estuary three-dimensional near-field hydrodynamic and transport modeling for entrainment. Prepared for Potomac Electric Power Company, Environmental Affairs Group, Water and Land Use Department, Washington, D. C., by J. E. Edinger Associates, Inc., Wayne, Pennsylvania.
- Eldridge, M. B. 1977. Factors influencing distribution of fish eggs and larvae over eight 24-hr samplings in Richardson Bay, California. *Calif. Fish and Game* 63:101-116.
- Fortier, L., and J. A. Gagné. 1990. Larval herring (*Clupea harengus*) dispersion, growth, and survival in the St. Lawrence estuary: match/mismatch or membership/vagrancy? *Can. J. Fish. Aquat. Sci.* 47:1898-1912.
- Fortier, L., and W. C. Leggett. 1982. Fickian transport and the dispersal of fish larvae in estuaries. *Can. J. Fish. Aquat. Sci.* 39:1150-1163.
- Giguère, L. A., J.-F. St-Pierre, B. Bernier, A. Vezina, and J.-G. Rondeau. 1989. Can we estimate the true weight of zooplankton samples after chemical preservation? *Can. J. Fish. Aquat. Sci.* 46:522-527.
- Graham, J. J., and D. B. Sampson. 1982. An experiment on factors affecting depth distribution of larval herring, *Clupea harengus*, in coastal Maine. *NAFO Sci. Count. Studies* 3:33-38.
- Greengrove, C. 1991. The physical oceanography of Port Moller, Alaska. Prepared for the U.S. National Oceanic and Atmospheric Administration, National Ocean Service, Anchorage, Alaska, by EG&G Washington Analytical Services Center, Inc., Waltham, Massachusetts.
- Heath, M. R., P. M. MacLachland, and J. H. A. Martin. 1987. Inshore circulation and transport of herring larvae off the north coast of Scotland. *Mar. Ecol. Prog. Ser.* 40:11-23.

- Heath, M. R., E. W. Henderson, and D. L. Baird. 1988. Vertical distribution of herring larvae in relation to physical mixing and illumination. *Mar. Ecol. Prog. Ser.* 47:211-228.
- Hjort, J. C. 1914. Fluctuations in the great fisheries of northern Europe. *Rapp. P.-v. Réun. Cons. int. Explor. Mer* 20:1-228.
- Holland, D. L., and B. E. Spencer. 1973. Biochemical changes in fed and starved oysters, *Ostrea edulis* L., during larval development, metamorphosis and early spat growth. *J. Mar. Biol. Assoc. U.K.* 53:287-298.
- Houde, E. D. 1977a. Abundance and potential yield of the round herring, *Etrumeus teres*, and aspects of its early life history in the eastern Gulf of Mexico. *Fish. Bull., U.S.* 75:61-89.
- Houde, E. D. 1977b. Abundance and potential yield of the Atlantic thread herring, *Opisthonema oglinum*, and aspects of its early life history in the eastern Gulf of Mexico. *Fish. Bull., U.S.* 75:493-512.
- Houde, E. D. 1977c. Abundance and potential yield of the scaled sardine, *Harengula jaguana*, and aspects of its early life history in the eastern Gulf of Mexico. *Fish. Bull., U.S.* 75:613-628.
- Iles, T. D., and M. Sinclair. 1982. Atlantic herring stock discreteness and abundance. *Science* 215:627-633.
- Kinder, T. H., and J. D. Schumacher. 1981. Hydrographic structure over the continental shelf of the southeastern Bering Sea. p. 31-52. *In* Hood, D. W., and J. A. Calder [eds.] *The eastern Bering Sea shelf: oceanography and resources*. Vol. I.
- Leak, J. C., and E. D. Houde. 1989. Cohort growth and survival of bay anchovy *Anchoa mitchilli* larvae in Biscayne bay, Florida. *Mar. Ecol. Prog. Ser.* 37: 109-122.

- Lenarz, W. H. 1973. Dependence of catch rates on size of fish larvae. Rapp. P.-v. Réun. Cons. int. Explor. Mer 164:270-275.
- McCullough, J. N. 1990. Alaska Peninsula and Aleutian Islands management areas sac roe herring report, 1990. Alaska Department of Fish and Game Regional Report 4K90-33, Division of Commercial Fisheries, 211 Mission Road, Kodiak, Alaska 99615. 30p.
- McGurk, M. D. 1989a. Advection, diffusion and mortality of Pacific herring larvae *Clupea harengus pallasii* in Bamfield Inlet, British Columbia. Mar. Ecol. Prog. Ser. 51:1-18.
- McGurk, M. D. 1989b. Early life history of Pacific herring in Auke Bay, Alaska: relationships of growth and survival to environmental conditions. U.S. Dep. Commerc., NOAA, OCSEAP Final Rep. 63:279-421.
- McGurk, M. D. 1989c. Early life history of Pacific herring: the 1989 Port Moller reconnaissance survey. U.S. Dep. Commerc., NOAA, OCSEAP Final Rep. 66:49-202.
- McGurk, M. D., J. E. Edinger, and E. M. Buchak. 1989. Early life history of Pacific herring: the 1989 Port Moller planning study. U.S. Dep. Commerc., NOAA, OCSEAP Final Rep. 66:1-48.
- McGurk, M. D., H. D. Warburton, J. E. Edinger, and E. M. Buchak. 1991. Fisheries oceanography of the southeast Bering Sea: relationships of growth, dispersion and mortality of herring larvae to environmental conditions in the Port Moller estuary. Appendices to the 1990 annual report. Prepared for the U.S. Minerals Management Service, Anchorage, Alaska, by Triton Environmental Consultants Ltd., Richmond, B. C., Canada.
- McGurk, M. D., H. D. Warburton, and V. Komori. 1990. Early life history of Pacific herring: Prince William Sound herring larvae survey. U.S. Dep. Commerc., NOAA, OCSEAP Final Rep. 71:151-237.

- Methot, R. D. 1986. Frame trawl for sampling pelagic juvenile fish. *CalCOFI Rep.* 27:267-278.
- Moller, H. 1984. Reduction of larval herring population by a jellyfish predator. *Science* 224:621-622.
- Morse, W. W. 1989. Matchability, growth, and mortality of larval fishes. *Fish. Bull., U.S.* 87:417-446.
- Munk, P., T. Kiorboe, and V. Christensen. 1989. Vertical migrations of herring, *Clupea harengus*, larvae in relation to light and prey distribution. *Env. Biol. Fishes* 26:87-98.
- Murphy, G. I., and R. I. Clutter. 1972. Sampling anchovy larvae with a plankton purse seine. *Fish. Bull., U.S.* 70:789-798.
- National Climatic Data Center. 1990. Local climatological data, monthly summary, Cold Bay, Alaska, April 1990 to August 1990, NOAA, Asheville, North Carolina.
- Okubo, A. 1980. Diffusion and ecological problems: mathematical models. Lecture notes in biomathematics; vol. 10. Springer-Verlag, Berlin. 254 p.
- Pearcy, W. G., and S. S. Myers. 1974. Larval fishes of Yaquina Bay, Oregon: a nursery ground for marine fishes? *Fish. Bull., U.S.* 72:201-213.
- Pearre, S., Jr. 1980. The copepod width-weight relation and its utility in food chain research. *Can. J. Zool.* 58:1884-1891.
- Robinson, D. G. 1969. Number, size composition, weight and food of larval and juvenile fish caught with a two-boat surface trawl in the Strait of Georgia July 4-6, 1967. *Fish. Res. Board Can. MS Rep. No. 1012: 71p.*
- Robinson, D. G., W. E. Barraclough, and J. D. Fulton. 1968a. Number, size composition, weight and food of larval and juvenile fish caught with a two-

- boat surface trawl in the Strait of Georgia May 1-4, 1967. Fish. Res. Board Can. MS Rep. No. 964: 105p.
- Robinson, D. G., W. E. Barraclough, and J. D. Fulton. 1968b. Number, size composition, weight and food of larval and juvenile fish caught with a two-boat surface trawl in the Strait of Georgia June 5-9, 1967. Fish. Res. Board Can. MS Rep. No. 72: 109p.
- Robinson, S. M. C. 1988. Early life history characteristics of Pacific herring, *Clupea harengus pallasii* Valenciennes 1847, in the Strait of Georgia, British Columbia: hydrodynamics, dispersal, and analysis of growth rates. Ph.D. thesis, University of British Columbia, Vancouver, B. C., 141p.
- Sameoto, D. D. 1984. Environmental factors influencing diurnal distribution of zooplankton and ichthyoplankton. J. Plankton Res. 6:767-792.
- Schnack, D., and G. Hempel. 1971. Notes on sampling herring larvae by Gulf III samplers. Rapp. P.-v. Réun. Cons. int. Explor. Mer 160:56-59.
- Seliverstov, A. A. 1974. Vertical migrations of larvae of Atlanto-Scandian herring (*Clupea harengus* L.). p. 253-261. In Blaxter, J. H. S. (ed.), The early life history of fish. Springer-Verlag, Berlin.
- Sprules, W. G., and M. Munawar. 1986. Plankton size spectra in relation to ecosystem productivity, size, and perturbation. Can. J. Fish. Aquat. Sci. 43: 1789-1794.
- Stephenson, R. L., and M. J. Power. 1988. Semidiel vertical movements in Atlantic herring *Clupea harengus* larvae: a mechanism for larval retention? Mar. Ecol. Prog. Ser. 50:3-11.
- Stevenson, J. C. 1962. Distribution and survival of herring larvae (*Clupea harengus* Valenciennes) in British Columbia waters. J. Fish. Res. Board Can. 19:735-810.

- Taggart, C. T., and W. C. Leggett. 1987. Short-term mortality in post-emergent larval capelin *Mallotus villosus*. II. Importance of food and predator density, and density-dependence. *Mar. Ecol. Prog. Ser.* 41:219-229.
- Tibbo, S. N., J. E. H. Legaré, L. W. Scattergood, and R. F. Temple. 1958. On the occurrence and distribution of larval herring (*Clupea harengus* L.) in the Bay of Fundy and the Gulf of Maine. *J. Fish. Res. Bd. Canada*, 15:1451-1469.
- Wailes, G. H. 1935. Food of *Clupea pallasii* in southern British Columbia waters. *J. Biol. Bull. Canada* 1:477-486.
- Ware, D. M., and T. C. Lambert. 1985. Early life history of Atlantic mackerel (*Scomber scombrus*) in the southern Gulf of St. Lawrence. *Can. J. Fish. Aquat. Sci.* 42:577-592.
- Weinstein, M. P., S. L. Weiss, R. G. Hodson, and L. R. Gerry. 1980. Retention of three taxa of postlarval fishes in an intensively flushed tidal estuary, Cape Fear River, North Carolina. *Fish. Bull., U.S.* 78:419-435.
- Wood, J. R. 1971. Some observations on the vertical distribution of herring larvae. *Rapp. P.-v. Réun. Cons. int. Explor. Mer* 160:60-64.
- Yin, M. C., and J. H. S. Blaxter. 1987. Escape speeds of marine fish during early development and starvation. *Mar. Biol.* 96:459-468.
- Zweifel, J. R., and P. E. Smith. 1981. Estimates of abundance and mortality of larval anchovies (195 1-75): application of a new method. *Rapp. P.-v. Réun. Cons. int. Explor. Mer* 178:248-259.

Table 1. Distances from plankton stations to the heads of Moller and Herendeen Bays.

Moller Bay		Herendeen Bay	
Station	Distance (km)	Station	Distance (km)
Frying Pan	0.0	Portage Creek	0.0
47	4.3	37	2.2
46	8.4	36	5.6
45	13.2	35	8.8
42	16.4	34	13.6
41	20.8	33	12.5
39	25.2	31	16.7
38	31.1	29	20.3
21	37.0	28	27.8
22	38.0	27	25.2
23	40.7		
48	41.0		
49	44.3		
25	37.1		
26	41.7		
27	47.4		
28	52.0		

Table 2. Commercial herring catch of the Port Moller area, 1982-1990, in metric tonnes (McCullough 1990).

Year	Deer Island	Herendeen Bay	Moller Bay	Bear River and Bering Sea coast	Total
1982	0.0	261.0	163.4	41.8	466.3
1983	0.0	472.6	32.7	73.5	578.8
1984	0.0	164.3	227.2	0.0	391.5
1985	66.3	90.8	232.4	260.6	650.1
1986	37.7	102.1	237.4	429.9	807.1
1987	0.0	146.0	312.6	6.6	465.3
1988	0.0	7.4	259.2	0.0	266.7
1989	0.0	60.8	105.6	509.8	676.2
1990	0.0	141.5	106.3	0.0	247.7
Mean	11.6	160.7	186.3	146.9	505.5
SD	24.0	136.8	89.9	201.7	189.1

Table 3. Commercial herring catch and percent roe in Port Moller in 1990.

Area	Date	Catch (t)	Percent roe
Upper Moller Bay	June 4	50.8	6.83
	June 5	19.0	7.85
	June 6	33.8	7.34
	June 10	2.7	7.71
Total		106.3	
Herendeen Bay	June 8	6.5	7.30
	June 11	11.6	7.90
	June 12	11.6	7.90
	June 13	9.8	8.50
	June 18	84.4	7.71
	June 19	17.4	7.80
Total		141.5	
Grand total		247.7	

Table 4. Aerial surveys of herring biomass in the Port Moller area in 1990 conducted by the Alaska Department of Fish and Game. Index of survey visibility: 1 = excellent; 2 = good; 3 = fair; 4 = poor; and 5 = unsatisfactory.

Date	Deer Island		Herendeen Bay		Moller Bay		Bear River	
	Tonnes	Index	Tonnes	Index	Tonnes	Index	Tonnes	Index
May 21					0	1	0	2
May 23	0	1	0	1	0	1	7	1
May 25					0	2	0	2
May 31							0	2
June 1	0	2	0	2	0	2	24	1
June 2					4	2	3	
June 5	0	3	0	3	0	3	0	3
June 7					34	2		
June 8	0	2	0	2				
June 10	0	3	28	3	35	2		
June 12	0	2	141	2	0	2		
June 14					351	2		

Table 5. Parameters of Gompertz growth models for eight sub-cohorts of herring larvae. Do is the day of year of hatch and n is the number of mean lengths at date. Brackets enclose one standard error of the parameters.

Sub-cohort	$A_0$ (mm·d <sup>-1</sup> )	a (mm·d <sup>-1</sup> )	Do	r <sup>2</sup>	n
1M	0.0216 (0.0067)	-0.0022 (0.0113)	146.3 (3.1)	0.90	17
1H	0.0462 (0.0031)	0.0314 (0.0051)	151.9 (0.5)	0.99	14
2M	0.0231 (0.0055)	-0.0033 (0.0102)	161.7 (1.9)	0.93	17
2H	0.0357 (0.0053)	0.0187 (0.0077)	163.6 (1.2)	0.98	15
3M	0.0191 (0.0132)	-0.0251 (0.0328)	174.9 (4.3)	0.78	11
3H	0.0298 (0.0076)	0.0004 (0.0133)	175.5 (2.0)	0.99	9
4M	0.0135 (0.0109)	-0.0414 (0.0420)	184.8 (4.6)	0.93	7
4H	0.0266 (0.0245)	-0.0283 (0.0674)	190.1 (5.1)	0.92	7

Table 6. Day of year of spawn and day of year of hatch (Do) for nine sub-cohorts of herring larvae. Dashes indicate no data available.

Cohort	Ageing method			Spawn date	Incubation time (d)
	Growth model	Yolk volume	Mean Do		
1M	146	149	147	124	23
1H	152	154	153	128	25
2M	162	165	163	148	15
2H	164	166	165	150	15
3M	175	176	175	162	13
3H	175	175	175	160	15
4M	185	189	187	176	11
4H	190	189	189	175	14
5M		205	205	196	11

Table 7. Vertical distribution of density ( $\text{number}\cdot\text{m}^{-3}$ ) of herring larvae at site 36 in Herendeen Bay on June 25-26. Depth of maximum density at each time is underlined.  $Z_{\text{cm}}$  is the center of mass, calculated for each length group.

Depth (m)	Mean hour of vertical series				
	1224	0053	0625	1216	1900
L = 9.0-14.9 mm					
0-10	0.176	<b>0123</b>	<b>0105</b>	<b>0117</b>	0211
10-20	<u>0307</u>	0.006	0.072	0.092	0.024
20-30	0.000	0.004	0.000	0.000	0.000
30-40	0.000	0.004	0.000	0.000	0.000
$Z_{\text{cm}}$	11.356	6.898	9.068	9.402	6.021
L $\geq$ 15 mm					
0-10	0.071	0133	<b>0153</b>	0.019	0.060
10-20	<b>0251</b>	0.040	0.078	<b>0180</b>	0102
20-30	0.000	0.000	0.000	0.000	0.010
30-40	0.000	0,000	0.000	0.000	0.000
$Z_{\text{cm}}$	12.795	7.312	8.377	14.045	12.092

Table 8. Vertical distribution of density (number·m<sup>-3</sup>) of herring larvae at site 39 in Møller Bay on July 2. Depth of maximum density at each time is underlined.  $Z_{cm}$  is the center of mass, calculated for each length group.

Depth (m)	Mean hour of vertical series							
	0017	0051	0555	0628	1208	1244	1816	1916
<b>L &lt; 9.0 mm</b>								
0-10	0.048	<u>0.142</u>	0.084	0.020	0.013	0.000	0.000	0.007
10-20	<u>0.090</u>	0.101	0.108	0.073	0.013	<u>0.096</u>	<u>0.040</u>	0.013
20-30	0.115	0.085	<u>0.225</u>	<u>0.130</u>	0.158	0.056	0.000	0.016
$Z_{cm}$	17.65	13.26	18.38	14.69	22.88	18.68	15.00	17.50
<b>L = 9.0-14.9 mm</b>								
0-10	<u>0.550</u>	0.327	0.533	0.325	0.212	<u>0.707</u>	0.600	0.375
10-20	0.681	<u>0.740</u>	<u>0.555</u>	<u>1.173</u>	0.319	0.635	<u>0.645</u>	<u>0.655</u>
20-30	<u>0.705</u>	0.500	0.448	0.334	<u>1.384</u>	0.320	0.393	0.377
$Z_{cm}$	15.80	16.10	14.45	15.05	21.12	12.67	13.74	15.01
<b>L ≥ 15.0 mm</b>								
0-10	0.000	0.009	0.000	0.000	0.005	0.000	0.000	0.000
10-20	<u>0.125</u>	0.000	<u>0.032</u>	0.000	0.008	<u>0.777</u>	0.016	0.017
20-30	0.000	<u>0.024</u>	0.016	<u>0.012</u>	<u>0.206</u>	0.042	0.031	0.019
$Z_{cm}$	15.00	19.55	18.33	25.00	24.18	18.53	21.59	20.28

Table 9. Vertical distribution of density ( $\text{number}\cdot\text{m}^{-3}$ ) of herring larvae at site 36 in Herendeen Bay on July 24-25. Depth of maximum density at each time is underlined.  $Z_{\text{cm}}$  is the center of mass, calculated for each length group.

Depth (m)	Mean hour of vertical series			
	1340	1900	0130	0700
<b>L = 9.0-15.0 mm</b>				
0-10	0.030	<i>0.072</i>	<i>0.103</i>	<i>0.209</i>
10-20	<u>0.280</u>	<i>0.204</i>	0.077	0.017
20-30	0.066	0.120	0.041	0.000
30-40	0.000	0.027	0.013	0.000
$Z_{\text{cm}}$	15.96	17.41	<i>13.46</i>	5.75
<b>L <math>\geq</math> 15.0 mm</b>				
0-10	0.000	0.048	<i>0.239</i>	<i>0.076</i>
10-20	<i>0.115</i>	0.034	<i>0.198</i>	0.035
20-30	0.051	0.234	<i>0.063</i>	0.061
30-40	0.000	<i>0.501</i>	0.009	0.032
$Z_{\text{cm}}$	18.07	29.54	11.90	17.40

Table 10. Locations of hatch sites of nine sub-cohorts of herring larvae from Port Moller in 1990. Distances are from the heads of the two bays.

Cohort	Moller Bay		Herendeen Bay	
	Distance (km)	nearest station	Distance (km)	nearest station
1	17.2	42	7.8	35
2	12.2	45	17.2	31
3	19.9	41	17.0	31
4	9.5	46	6.9	36
5	15.5	42		

Table 11. Mean spatial variance,  $s_{xt}^2$  (m<sup>2</sup>), of larval herring density.

Position	Moller Bay	Herendeen Bay
Seaward	mean = 13.2956 · 10 <sup>7</sup> SD = 7.2779 · 10 <sup>7</sup> n = 21	mean = 4.9526 · 10 <sup>7</sup> SD = 3.8444 · 10 <sup>7</sup> n = 18
Anti-seaward	mean = 5.7190 · 10 <sup>7</sup> SD = 2.8154 · 10 <sup>7</sup> n = 13	mean = 4.4293 · 10 <sup>7</sup> SD = 3.0690 · 10 <sup>7</sup> n = 14

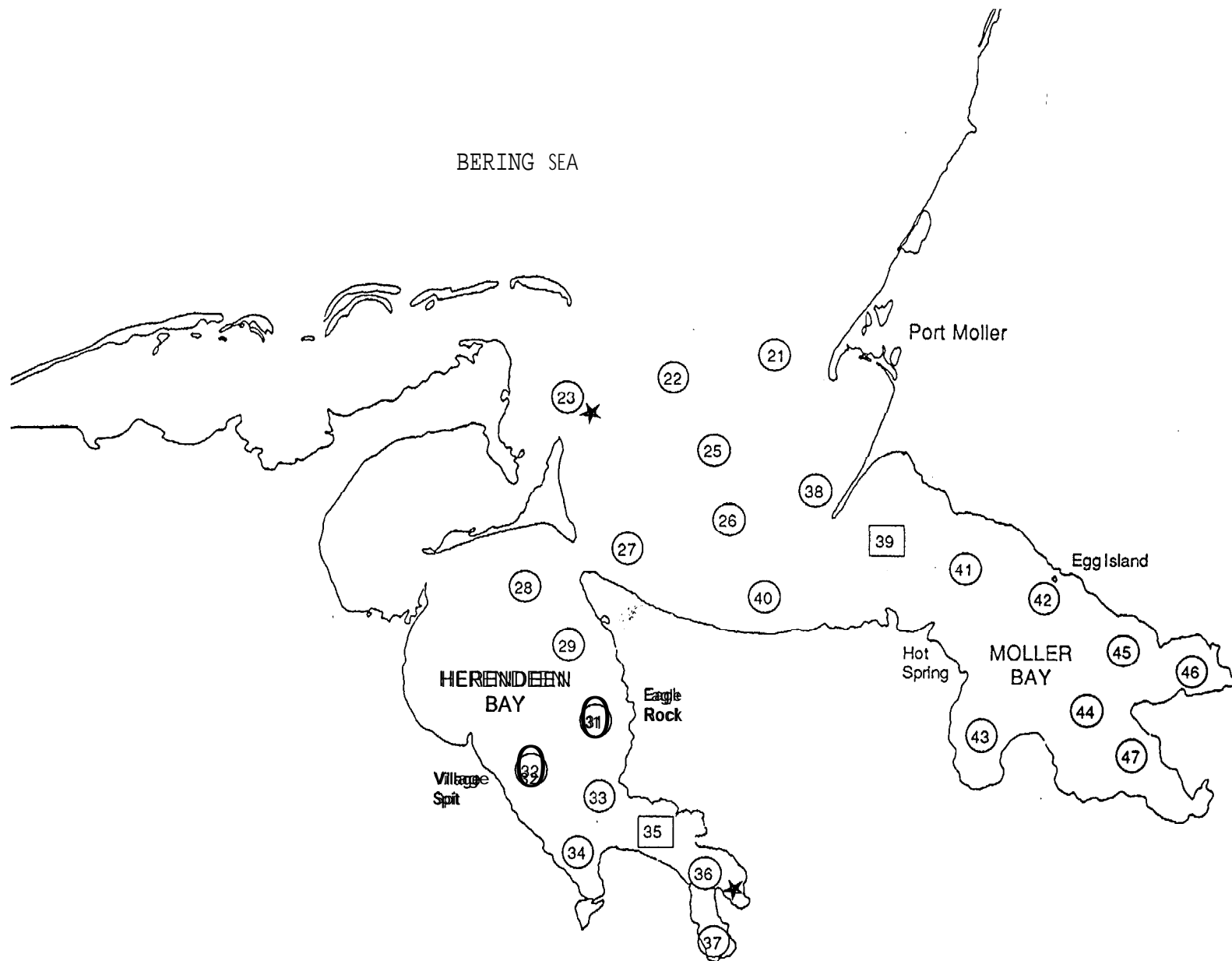


Fig. 1. Map of Port Moller estuary. Circled numbers indicate plankton stations. Boxes indicate stations at which microzooplankton samples and Tucker trawl samples were taken. Stars indicate water pressure sensors.

Velocity (cm) in Moller Bay (5/19/90)

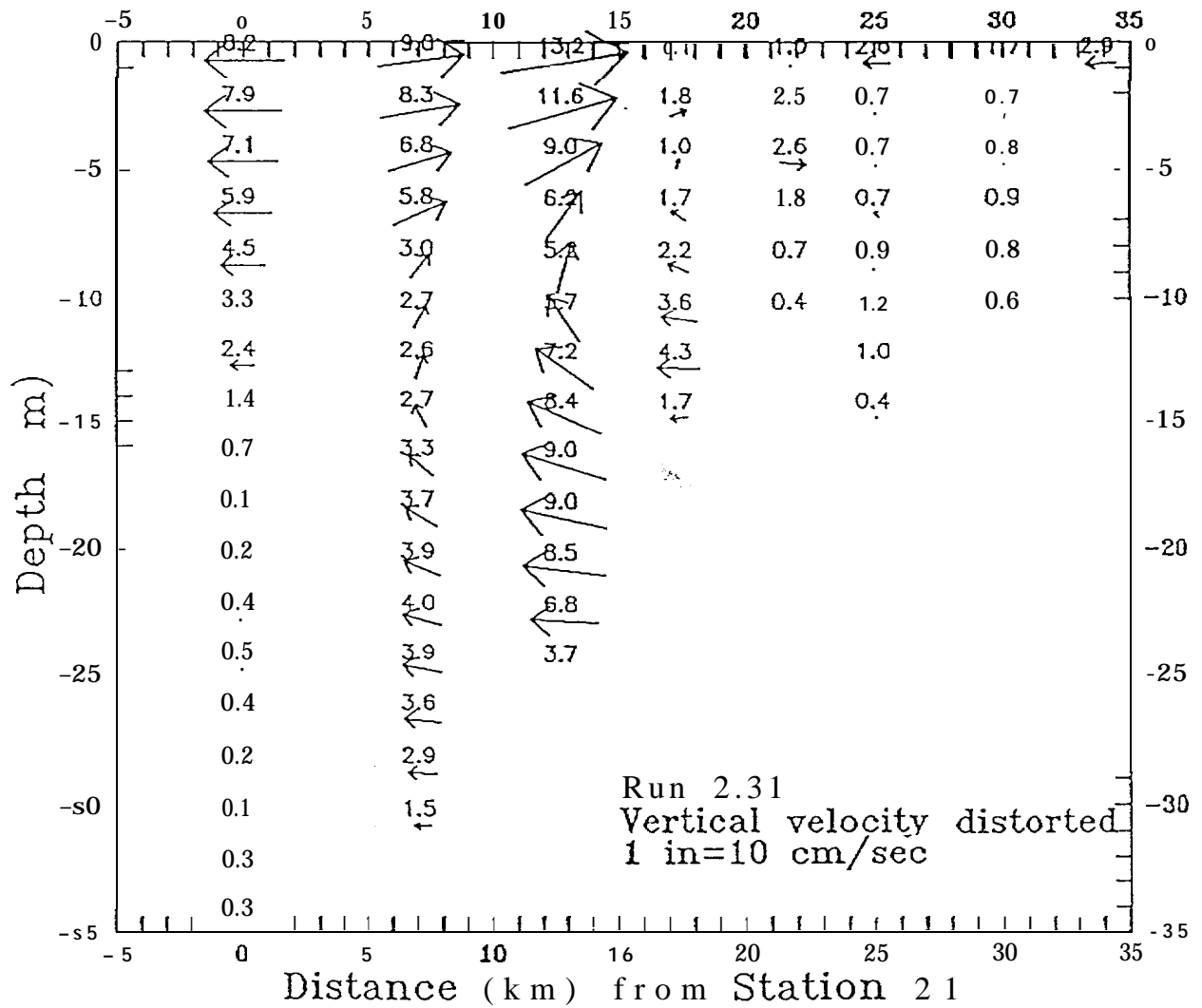


Fig. 2. Longitudinal-vertical plot of average water velocities in Moller Bay for May 12-19, 1990.

Velocity (cm) in Herendeen Bay (5/19/90)

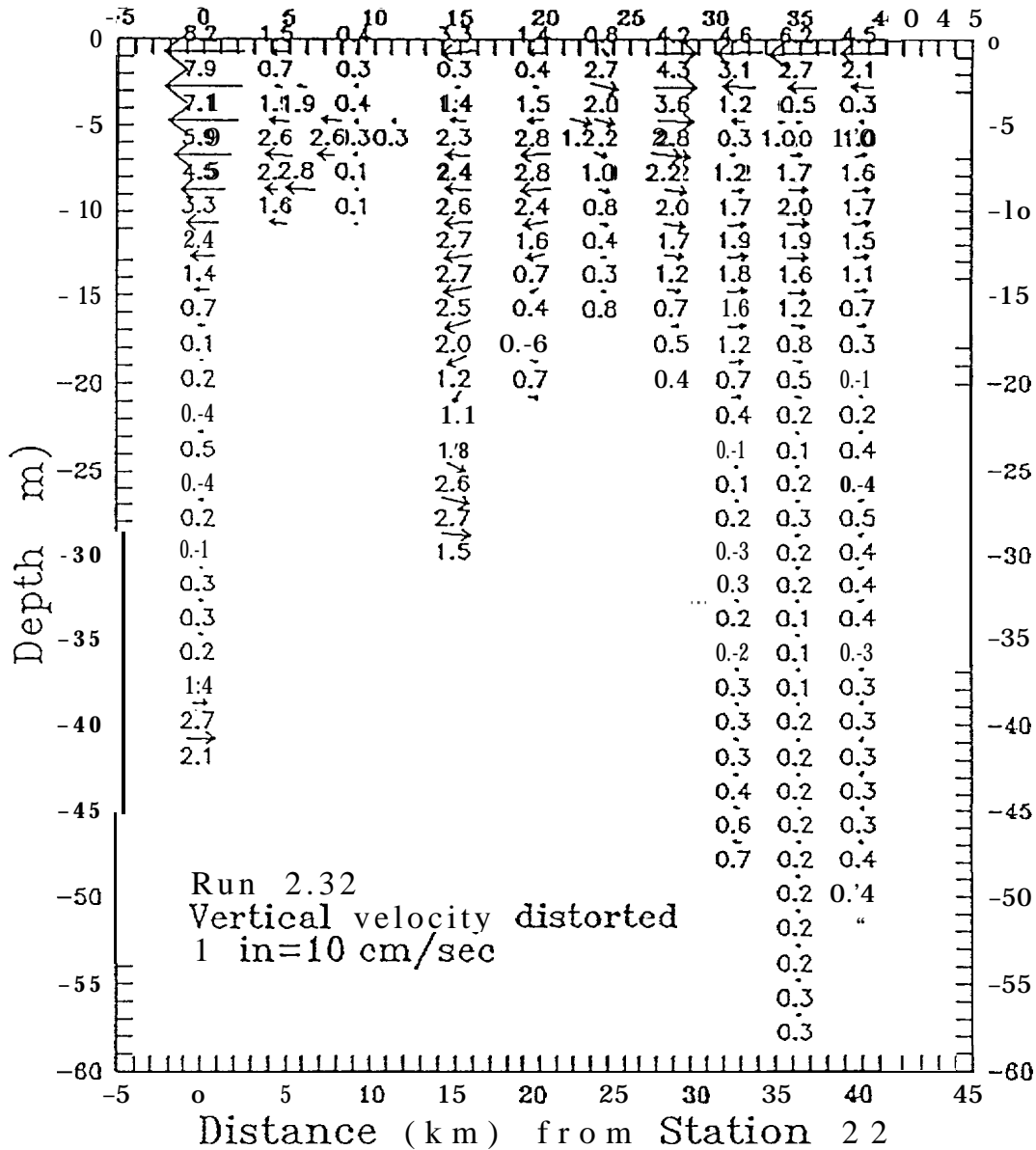


Fig. 3 Longitudinal-vertical plot of average water velocities in Herendeen Bay for May 12-19, 1990.

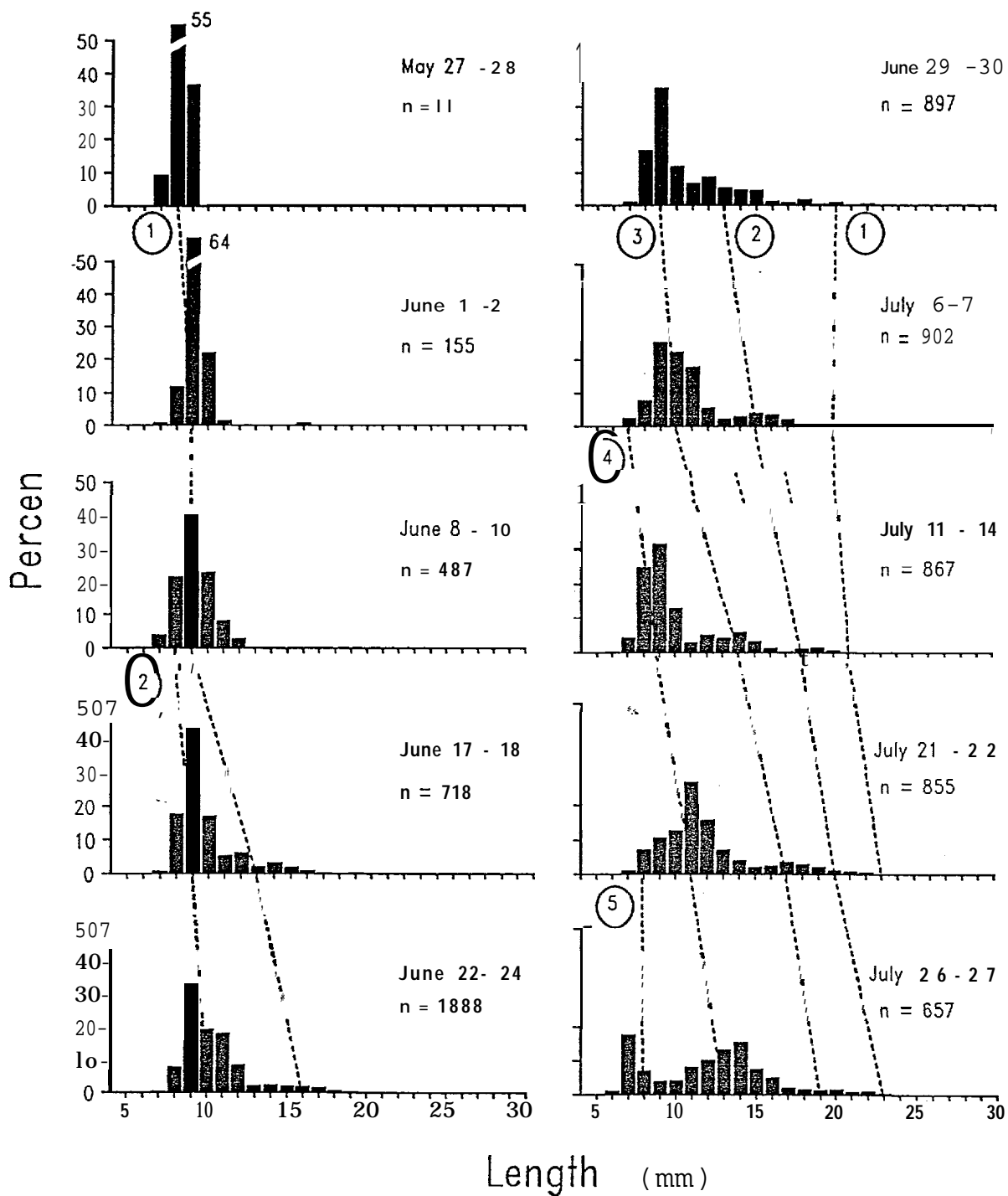


Fig. 4. Length frequency distributions at date for five cohorts of herring larvae found in Port Moller. Each cohort is identified by a circled number and by a broken line connecting mean lengths at date.

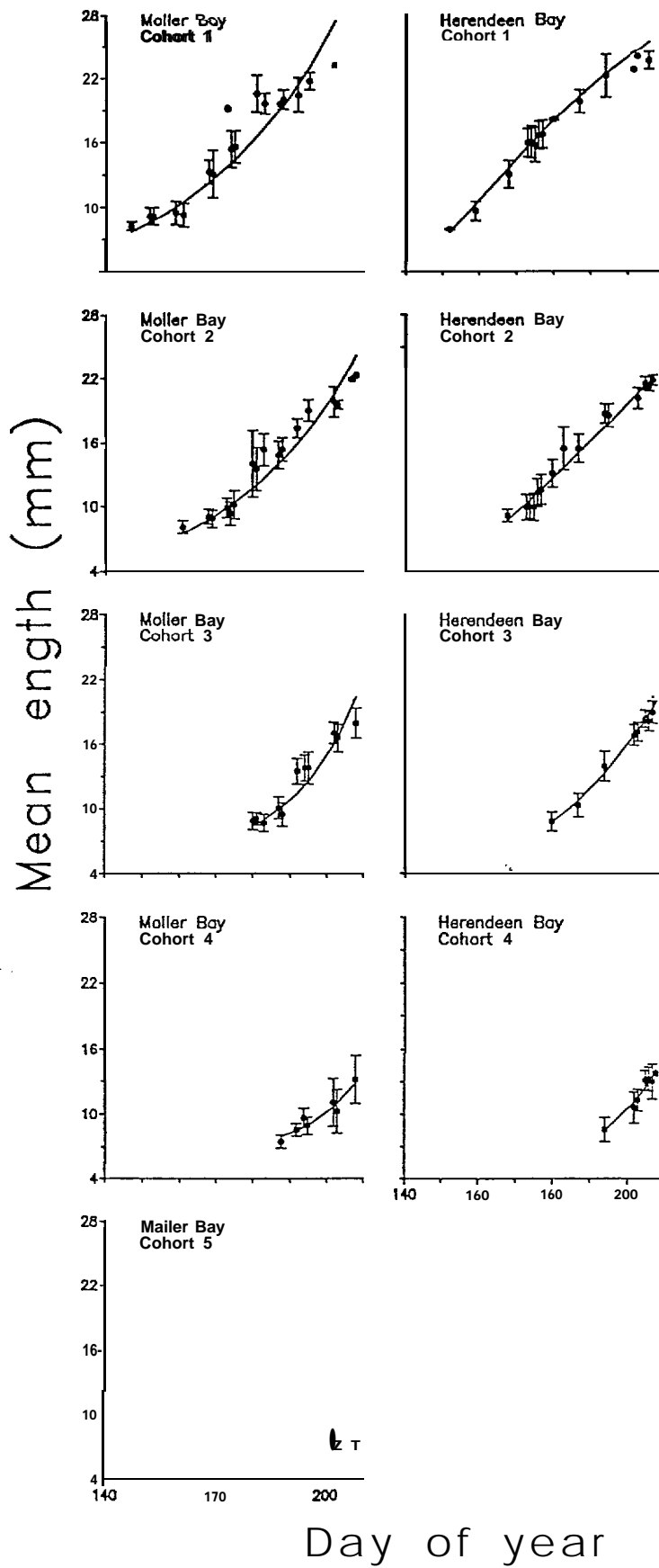


Fig. 5. Mean lengths ( $\pm 1$  SD) at day of year for nine sub-cohorts of herring larvae. Curves are lengths predicted by Gompertz growth models of Table 5.

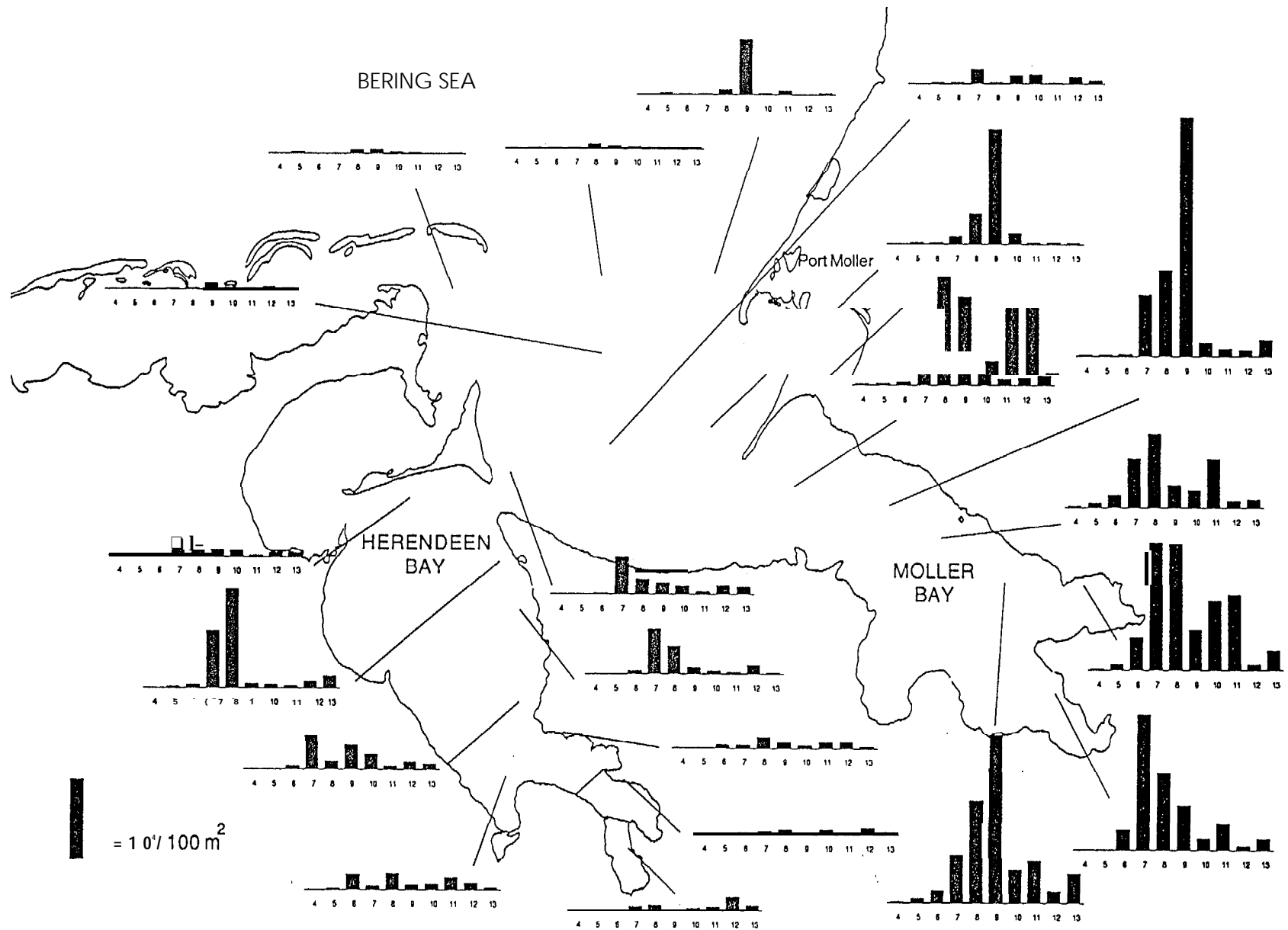


Fig. 6, Measured density (numbers·m<sup>-2</sup>) of herring larvae in the Port Moller estuary over May-July, 1990, as measured by bongo nets. Densities are not corrected for extrusion or net avoidance.

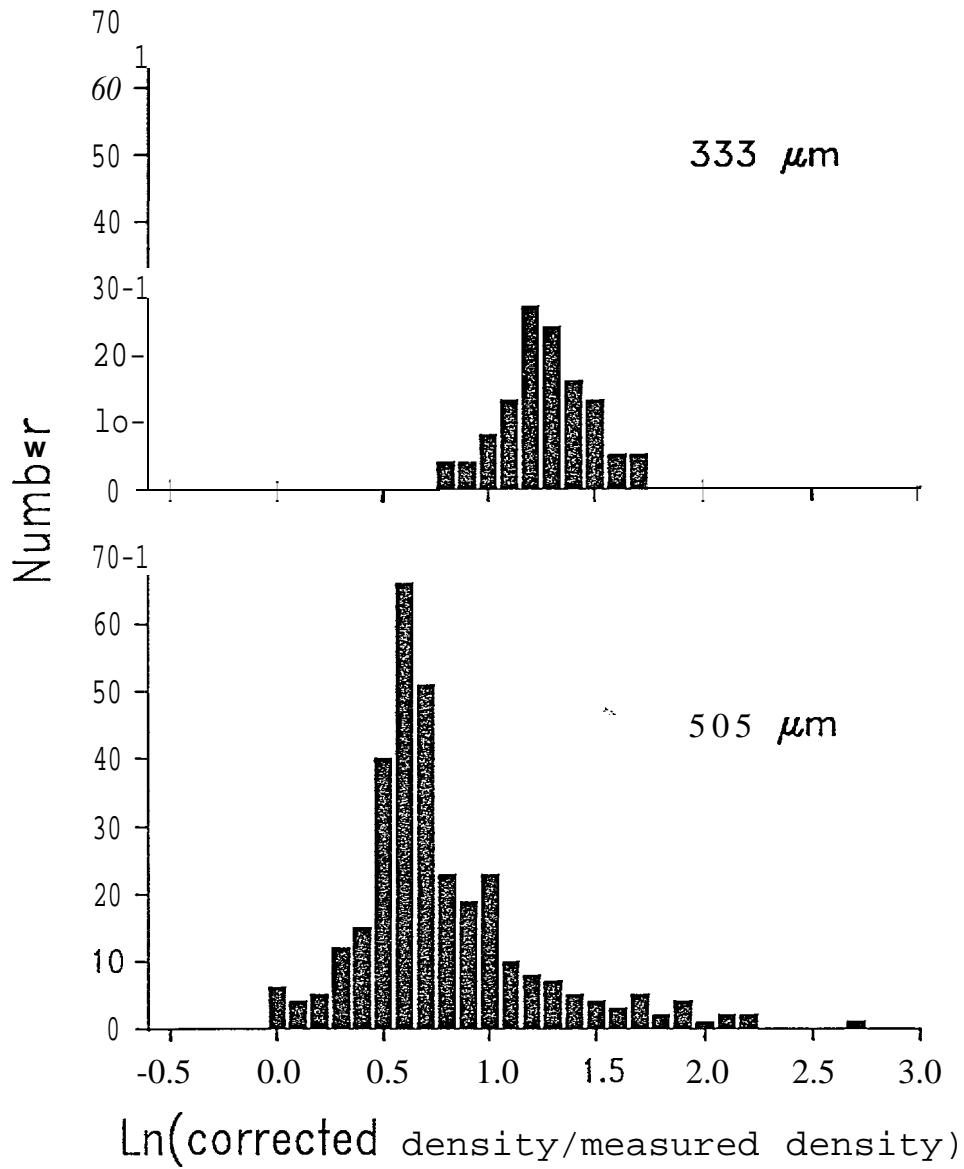


Fig. 7. Distribution of the In-transformed factor used to correct densities of herring larvae measured by bongo nets for net avoidance. Corrected-measured ratios are shown for the two mesh sizes of the bongo net.

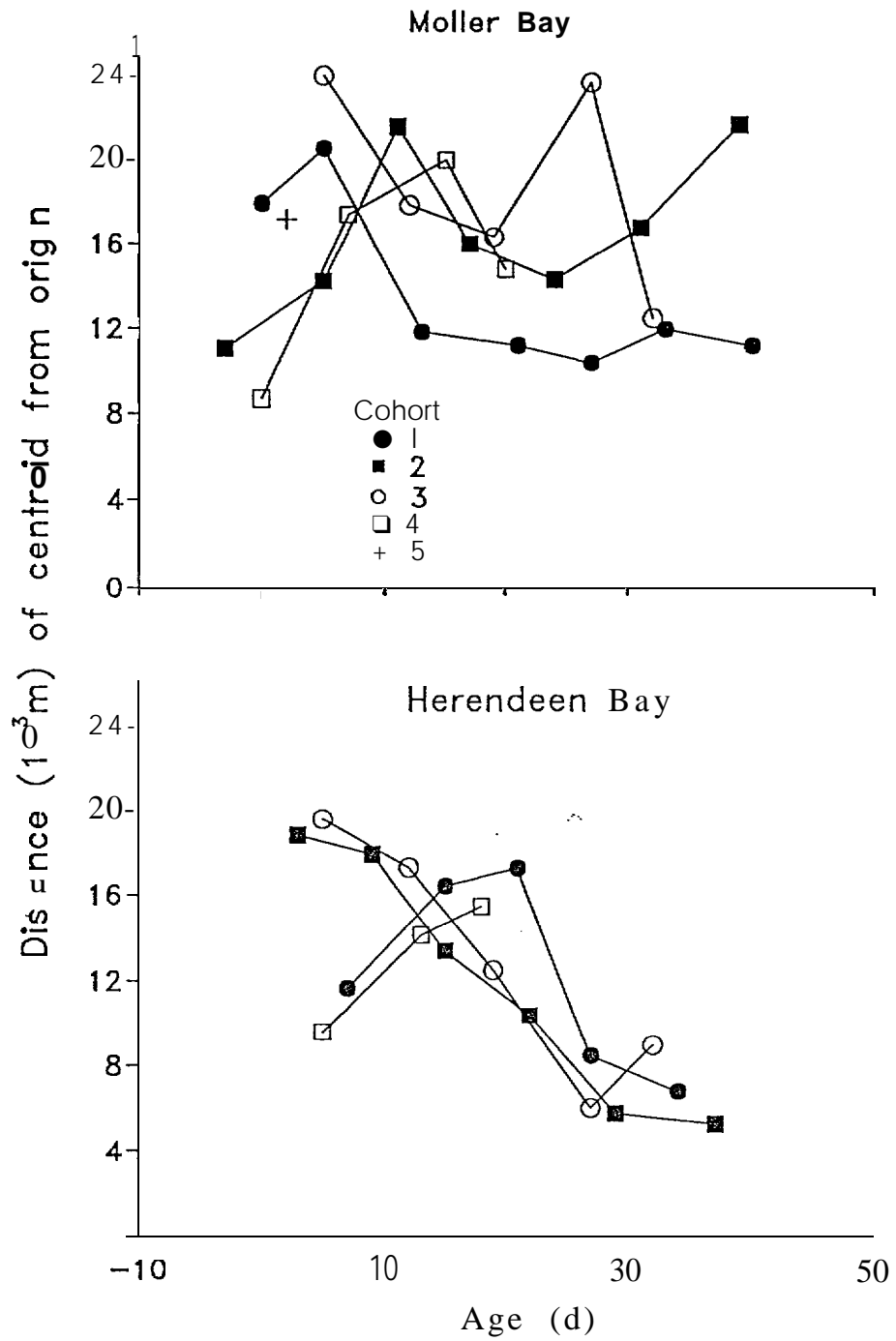


Fig. 8. The distances from the heads of Moller and Herendeen Bays to the centroids of nine sub-cohorts of herring larvae.

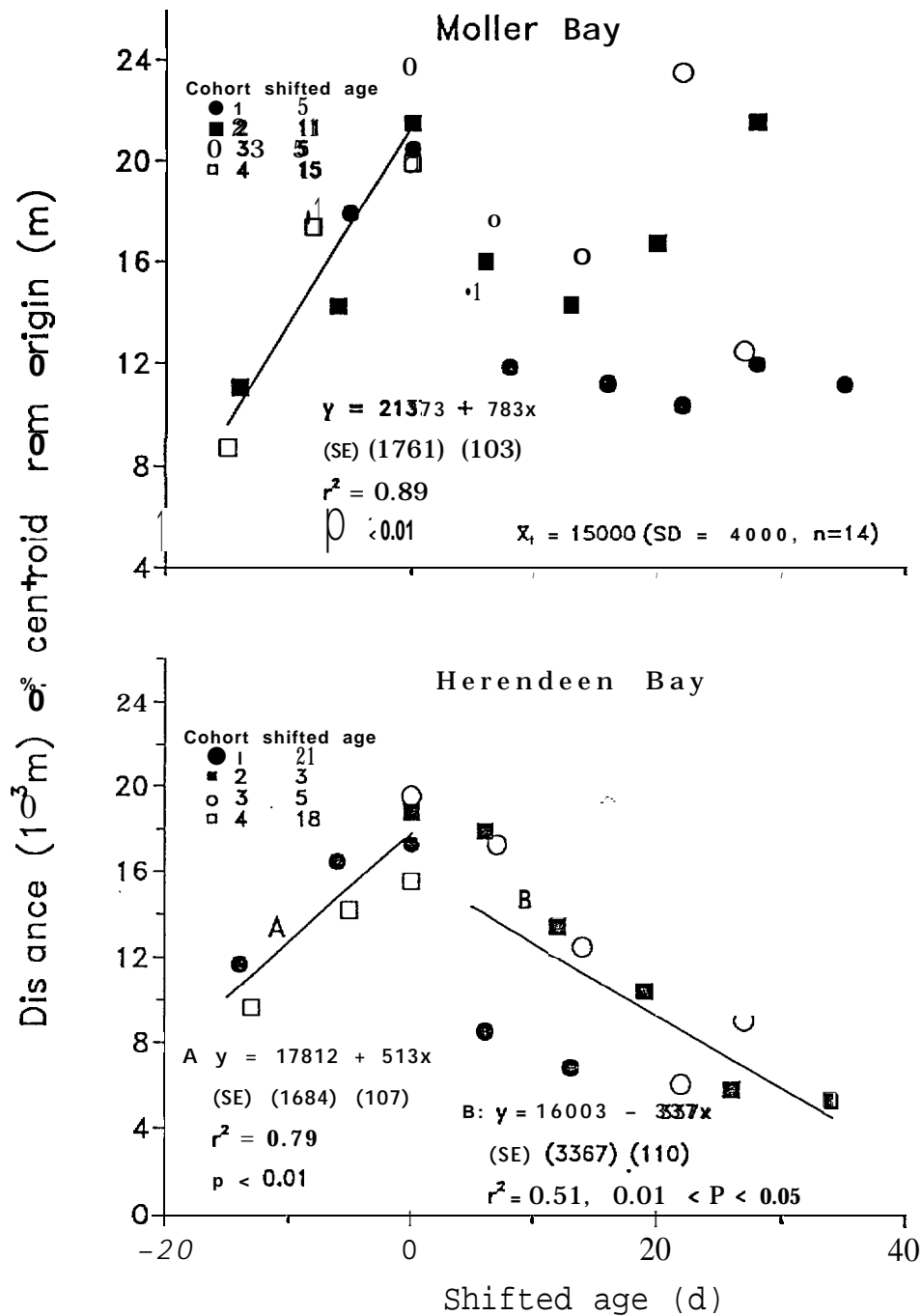


Fig. 9. Regressions of the centroids of eight sub-cohorts of larval herring on shifted age. Shifted age was true age minus the number of days between hatch and maximum distance from the head of a bay that the centroid of a sub-cohort ever reached.

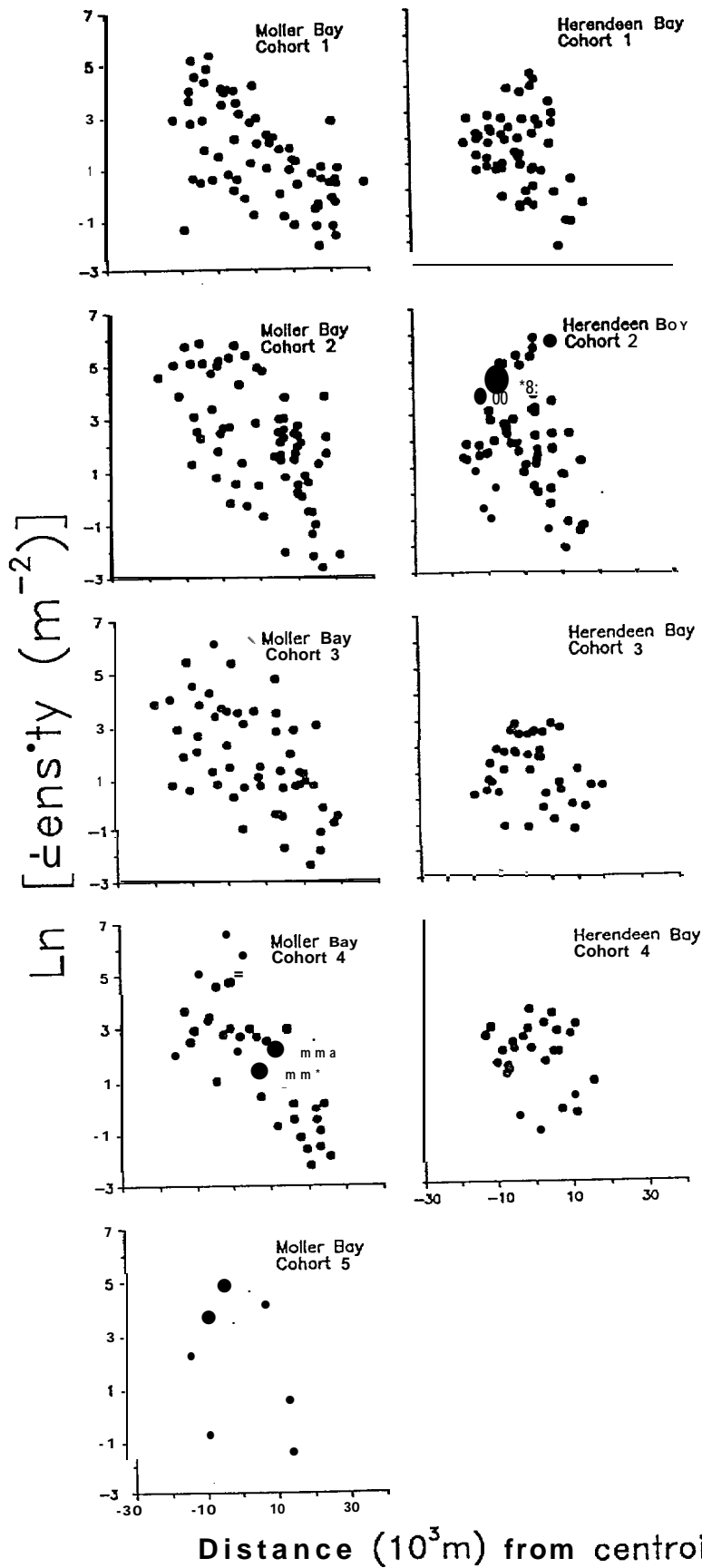


Fig. 10. Plots of  $\ln(\text{density})$  of herring larvae against the distance between a station and a centroid.

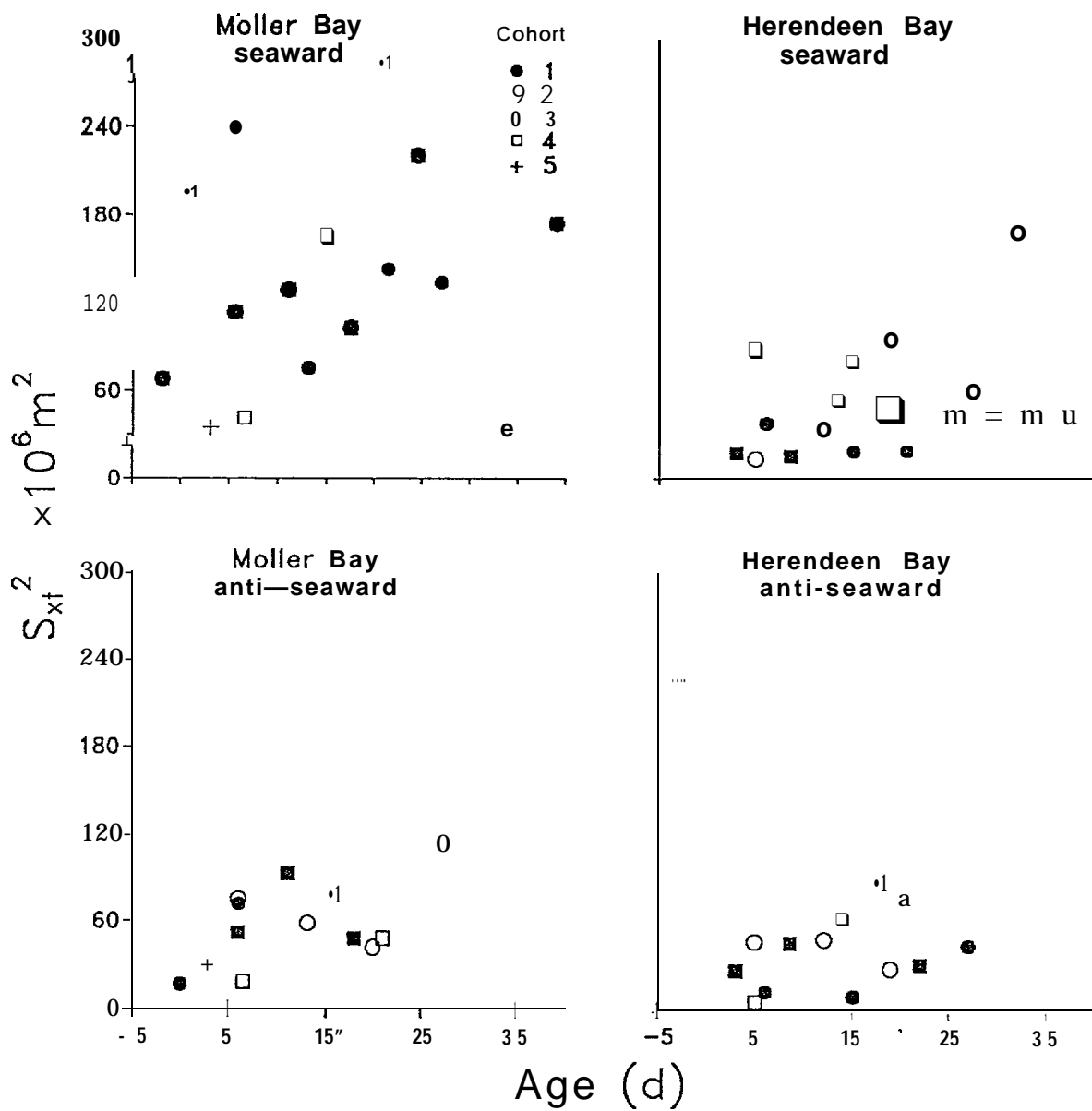


Fig. 11. Change in spatial variance of larval density with age for nine sub-cohorts of herring larvae.

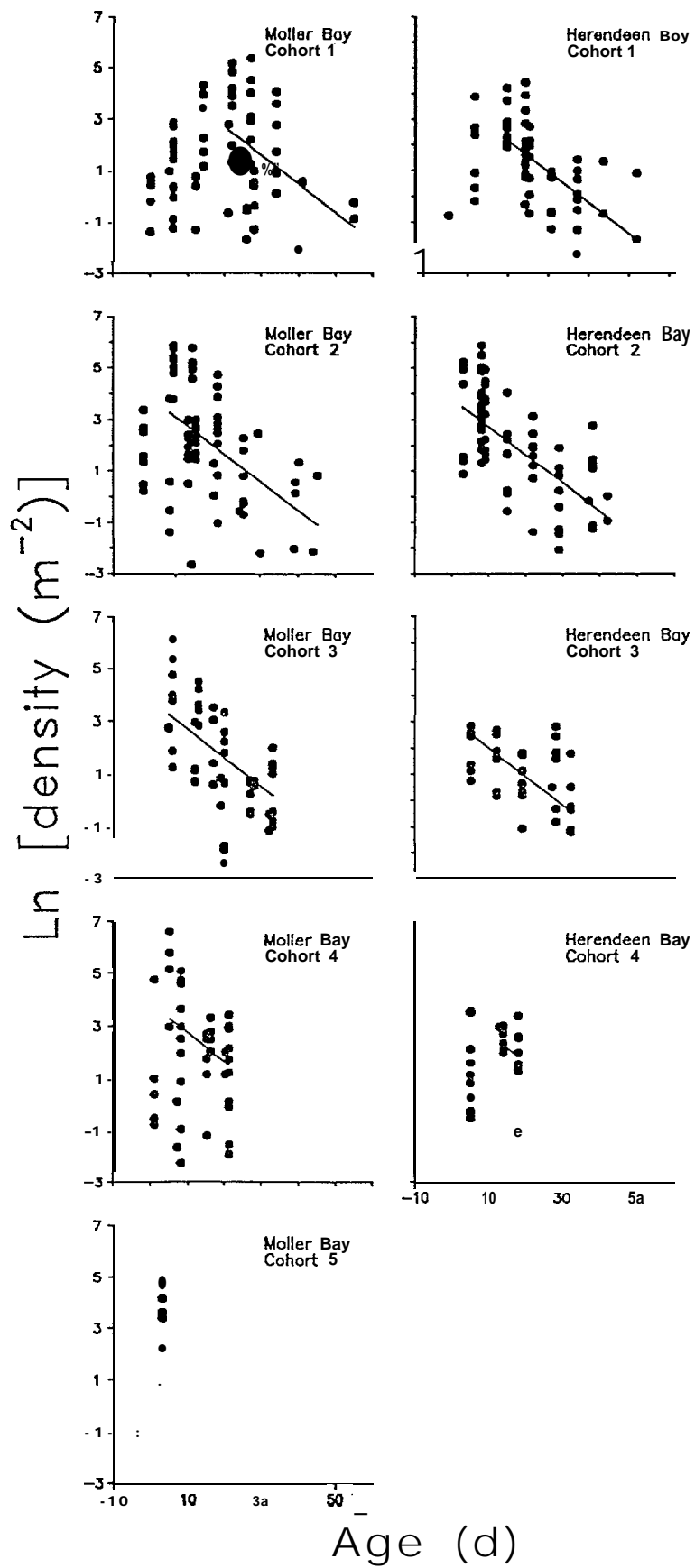


Fig. 12. Plots of  $\ln(\text{density})$  against age for nine sub-cohorts of herring larvae. Solid lines are predicted  $\ln(\text{density})$  from equation (15).

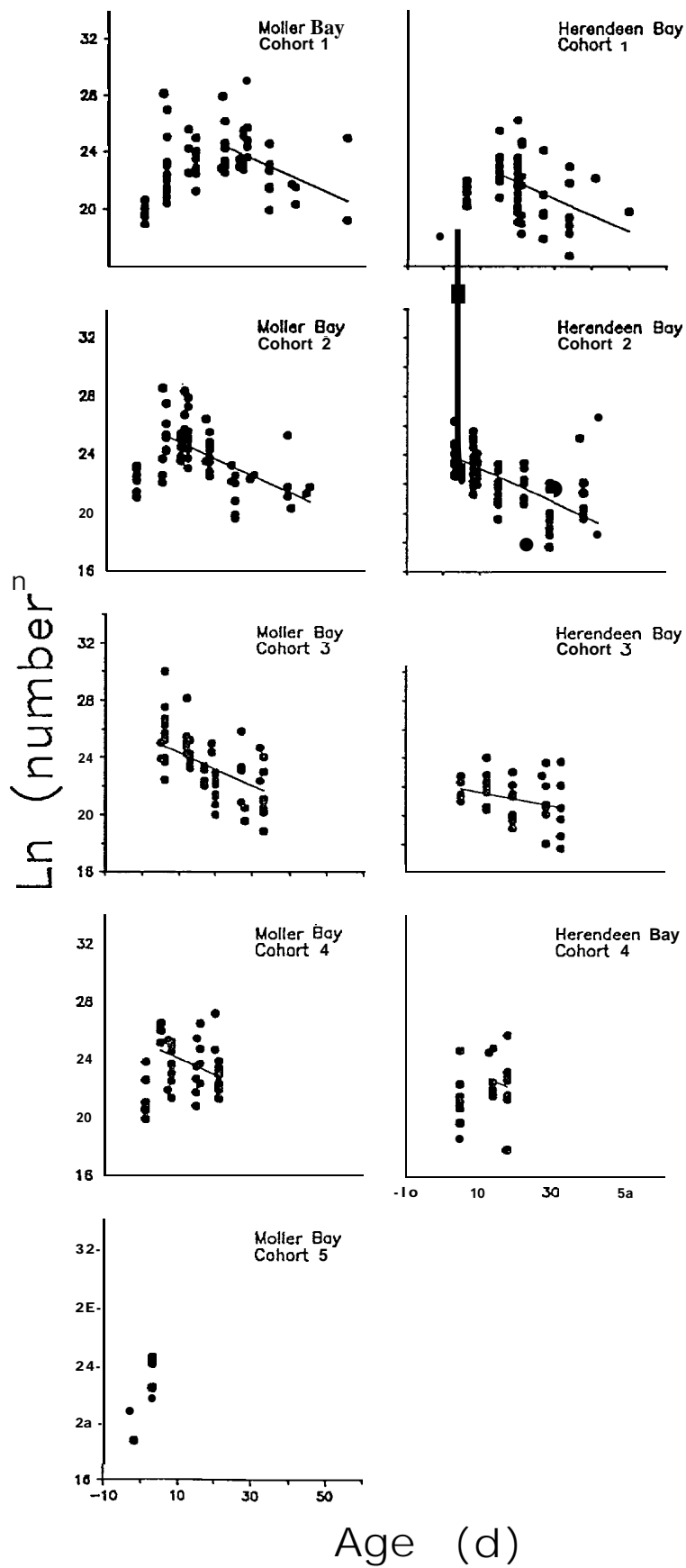


Fig. 13. Plots of  $\ln(\text{number})$  against age for nine sub-cohorts of herring larvae. Solid lines are predicted  $\ln(\text{number})$  from equation (16).